

A Comprehensive Survey on Video Scene Parsing: Advances, Challenges, and Prospects

Guohuan Xie, Syed Ariff Syed Hesham, Wenya Guo, Bing Li, Ming-Ming Cheng, Guolei Sun, and Yun Liu

Abstract—Video Scene Parsing (VSP) has emerged as a cornerstone in computer vision, facilitating the simultaneous segmentation, recognition, and tracking of diverse visual entities in dynamic scenes. In this survey, we present a holistic review of recent advances in VSP, covering a wide array of vision tasks, including Video Semantic Segmentation (VSS), Video Instance Segmentation (VIS), Video Panoptic Segmentation (VPS), as well as Video Tracking & Segmentation (VTS), and Open-Vocabulary Video Segmentation (OVVS). We systematically analyze the evolution from traditional hand-crafted features to modern deep learning paradigms—spanning from fully convolutional networks to the latest transformer-based architectures—and assess their effectiveness in capturing both local and global temporal contexts. Furthermore, our review critically discusses the technical challenges, ranging from maintaining temporal consistency to handling complex scene dynamics, and offers a comprehensive comparative study of datasets and evaluation metrics that have shaped current benchmarking standards. By distilling the key contributions and shortcomings of state-of-the-art methodologies, this survey highlights emerging trends and prospective research directions that promise to further elevate the robustness and adaptability of VSP in real-world applications.

Index Terms—Video Scene Parsing, Video Segmentation, Video Tracking, Open-Vocabulary, Deep Learning

1 INTRODUCTION

VIDEO Scene Parsing (VSP) is a fundamental problem in computer vision, aimed at assigning a semantic label to each pixel in a video sequence. It includes key tasks such as Video Semantic Segmentation (VSS), Video Instance Segmentation (VIS), and Video Panoptic Segmentation (VPS). By bridging the gap between static image analysis [1] and dynamic scene understanding [2], VSP plays a vital role in both academic research and industrial applications. Academically, VSP poses unique challenges, such as ensuring temporal consistency across frames [3]–[5], effectively extracting spatiotemporal features [6], [7], and accurately tracking dynamic objects in complex environments [8]. Addressing these challenges not only advances the theoretical foundations of computer vision but also drives innovation in related domains like pattern recognition and machine learning. From an industrial perspective, VSP underpins a wide range of critical applications, including autonomous driving, intelligent surveillance, robotics, and video editing. The ability to understand and interpret dynamic visual scenes is essential for enhancing decision-making processes and enabling robust performance in real-world scenarios.

Historically, early efforts in VSP relied heavily on hand-crafted features such as color histograms, texture descriptions, and optical flow [9]–[11], as well as classical machine learning models. Among these were clustering methods [12], graph-based approaches [13], support vector machines (SVMs) [14], random forests [15], and probabilistic graphical models like Markov

random fields and conditional random fields [16], [17]. While these foundational techniques laid the groundwork for the field, their limited scalability and reliance on domain-specific feature engineering hindered their applicability to complex video data.

The advent of deep learning, particularly Fully Convolutional Networks (FCNs) [1], [18]–[20], marked a substantial paradigm shift in the field of VSP. FCNs, with their ability to learn hierarchical feature representations and predict pixel-level labels, have significantly enhanced the accuracy and efficiency of VSP tasks. Over the last decade, FCN-based methods [21]–[25] have emerged as the dominant approach, establishing new benchmarks and demonstrating their versatility across various VSP scenarios.

Building upon the advancements of deep learning, the rise of transformer architectures [26] has further revolutionized the landscape of computer vision [27]–[35]. Originally developed for natural language processing (NLP), transformers [26] introduced the self-attention mechanism, which excels at capturing long-range dependencies and contextual relationships. Inspired by their success in NLP, vision transformers (*e.g.*, ViT [36], DETR [37]) have been adapted for visual tasks, thereby redefining the state-of-the-art in image and video segmentation. These transformer-based models leverage self-attention to model global interactions across spatial and temporal dimensions, overcoming the locality constraints of traditional Convolutional Neural Networks (CNNs) and paving the way for innovation in VSP.

In response to these technological advancements, the scope of VSP has broadened significantly to encompass increasingly sophisticated tasks. Video Tracking & Segmentation (VTS) represents a critical extension where the objective is not only to segment objects but also to maintain their identities consistently across frames [38], [39]. This task demands robust association strategies and the ability to handle occlusions, abrupt motion changes, and complex interactions, making it indispensable for applications such as multi-object tracking in crowded scenes and advanced video editing workflows.

- G. Xie, W. Guo, M.M. Cheng, G. Sun, and Y. Liu are with the College of Computer Science, Nankai University, Tianjin 300350, China.
- S. Hesham is with the School of Electrical and Electronic Engineering, Nanyang Technological University, Singapore 639798, as well as the Institute for Infocomm Research, A*STAR, Singapore 138632.
- Bing Li is with the School of Information and Communication Engineering, University of Electronic Science and Technology of China, Chengdu 611731, Sichuan, China.
- Corresponding author: Yun Liu (E-mail: liuyun@nankai.edu.cn)

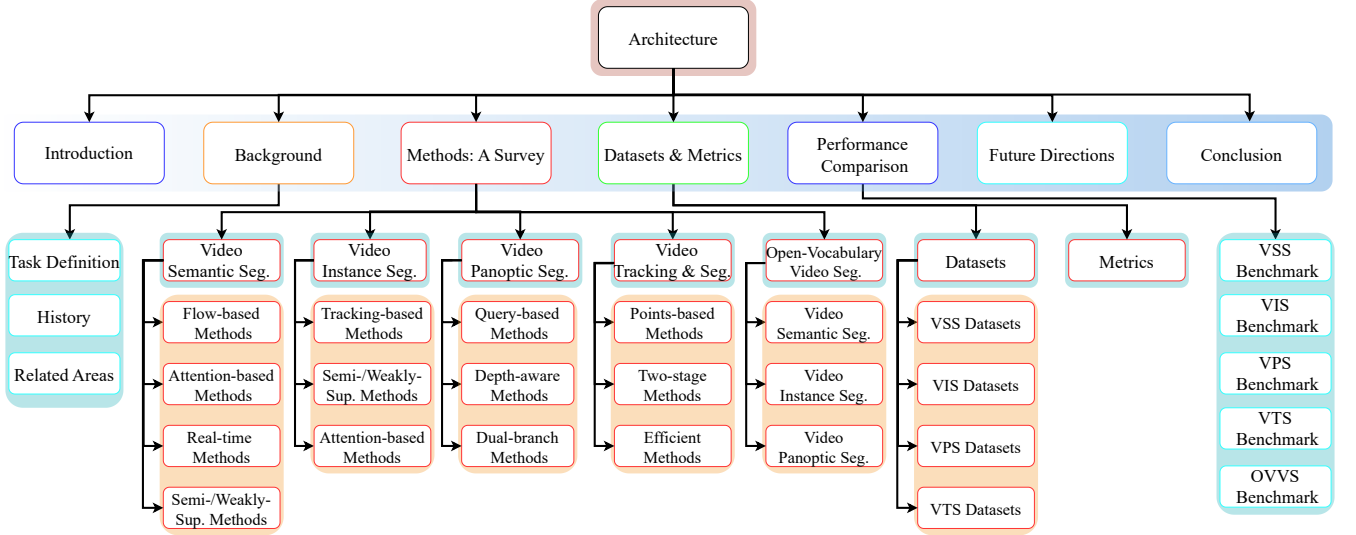


Fig. 1. Structure of this survey. The second row corresponds to seven sections.

Another emerging frontier is Open-Vocabulary Video Segmentation (OVVS), which integrates the CLIP model [40] to transcend the limitations of fixed label sets in VSS. By leveraging multi-modal learning and natural language cues, open-vocabulary approaches [41]–[45] empower systems to segment objects beyond predefined categories, thereby accommodating the vast diversity of objects encountered in real-world videos. This paradigm shift is particularly relevant in dynamic environments where new or rare objects frequently appear, demanding models that are both adaptable and capable of zero-shot generalization.

In light of these advancements, our survey provides a systematic exploration of the multifaceted progress in VSP. Unlike existing surveys that often emphasize specific subfields or techniques, our work bridges the gap between convolutional and transformer-based methodologies while adopting a unified perspective that encompasses VSS, VIS, VPS, VTS, and OVVS. Previous surveys, such as [46], have primarily focused on Video Object Segmentation (VOS), offering limited coverage of semantic, instance, and panoptic segmentation—key components for a holistic understanding of VSP. Similarly, the work in [47] centers extensively on transformer architectures, often sidelining convolution-based approaches that remain foundational to this field. By highlighting these shortcomings, our survey not only synthesizes the entire spectrum of VSP techniques but also critically assesses the evolution of both convolution- and transformer-based methods.

By addressing both longstanding challenges, such as temporal consistency and dynamic scene interpretation, and emerging demands like tracking, segmentation, and open-vocabulary recognition, this survey offers a comprehensive overview of the current state-of-the-art while laying the groundwork for future research directions. The integration of these diverse tasks reflects the natural progression of VSP towards a more holistic understanding of dynamic environments, ultimately driving innovations that are critical for real-world applications.

2 BACKGROUND

In this section, we first provide a formalized definition for the three primary tasks in Video Scene Parsing (VSP): Video Semantic

Segmentation (VSS), Video Instance Segmentation (VIS), and Video Panoptic Segmentation (VPS). We also include definitions for Video Tracking & Segmentation (VTS), as well as Open-Vocabulary Video Segmentation (OVVS), which are emerging tasks that expand the scope of VSP. This classification clarifies the scope and focus of VSS research §2.1. Subsequently, we present an overview of the history of VSP in §2.2. Finally, in §2.3, we introduce several related research areas that intersect with VSP.

2.1 Task Definition

To establish a framework for understanding the various tasks, let X and Y represent the input and output segmentation spaces, respectively. Deep learning-based approaches for video segmentation aim to learn an optimal mapping function $f^* : X \rightarrow Y$, where the objective is to map video data to the corresponding segmentation labels. Visual examples summarizing the differences among VSS, VIS, VPS, VTS, and OVVS with $T = 4$ are presented in Fig. 2.

Video Semantic Segmentation (VSS). The task of VSS focuses on predicting pixel-wise segmentation masks for each frame in a video clip $V \in \mathbb{R}^{T \times H \times W \times 3}$, where T represents the number of frames, H is the height, W is the width, and the last dimension represents color channels. These masks classify each pixel into predefined semantic categories such as road, sky, person, and so on, without distinguishing individual object instances. Notably, VSS does not require assigning unique IDs to objects or maintaining temporal consistency for object tracking.

Video Instance Segmentation (VIS). VIS builds upon VSS by incorporating instance-level masks associated with each object within the video. In this task, each object instance receives a unique ID, facilitating instance tracking across frames. The input video $V \in \mathbb{R}^{T \times H \times W \times 3}$ is segmented into a set of object masks $\{(m_i, c_i)\}_{i=1}^N$, where $m_i \in \{0, 1\}^{T \times H \times W}$ denotes the mask for the i -th instance, and c_i represents its class label. VIS necessitates maintaining temporal consistency in tracking each instance throughout the video.

Video Panoptic Segmentation (VPS). VPS further merges the objectives of VSS and VIS by jointly predicting segmentation

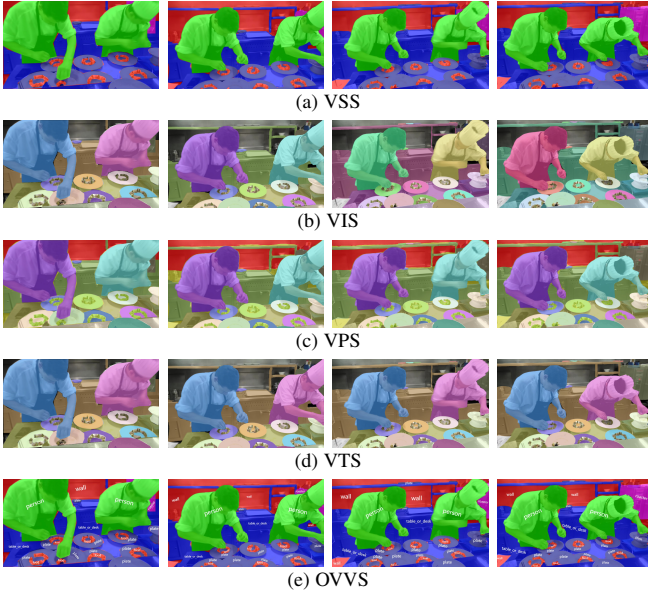


Fig. 2. **Illustration of different VSP tasks.** The examples are sampled from the VIPSeg dataset [48]. For VSS, the same color indicates the same semantic class across the entire video frame, without distinguishing instances. For VIS and VPS, different object instances are represented by different colors, with VPS further including both foreground instances and background semantics. VTS maintains consistent segmentation and tracking results for all pixels, culminating in a comprehensive segmentation output that captures both “things” and “stuff”. OVVS supports segmenting novel object categories beyond the predefined label set, with category names overlaid on each segment for clarity.

masks for both “stuff” (*e.g.*, amorphous regions like roads or skies) and “thing” (*i.e.*, countable object instances such as cars and people) classes. Each “thing” mask is attributed a unique ID for tracking purposes, while “stuff” masks do not require unique identifiers. VPS requires temporally consistent segmentation and tracking results for all pixels, culminating in a comprehensive segmentation output that captures both “things” and “stuff”.

Video Tracking & Segmentation (VTS). This task is an integrated approach where both pixel-level segmentation and temporal tracking of objects across frames are performed. Given a video clip input as $V \in \mathbb{R}^{T \times H \times W \times 3}$, VTS predicts segmentation masks for each object and assigns unique instance IDs to ensure consistent tracking over time. The output consists of object masks represented as $\{(m_i, c_i, id_i)\}_{i=1}^N$, where each mask $m_i \in \{0, 1\}^{T \times H \times W}$ corresponds to the i -th object, c_i denotes its class label, and id_i represents its unique identity. This formulation effectively addresses challenges such as object motion, occlusion, and appearance variations across frames.

Open-Vocabulary Video Segmentation (OVVS). OVVS broadens the traditional scope of VSS by removing the constraint of a fixed label set. For a given video clip $V \in \mathbb{R}^{T \times H \times W \times 3}$, the goal of OVVS is to generate pixel-level segmentation masks while assigning semantic labels derived from an open vocabulary, thereby accommodating both seen and unseen categories. This approach accommodates both seen and unseen categories, leveraging large-scale pre-trained models and cross-modal learning frameworks. As a result, OVVS significantly enhances the adaptability of video segmentation methods in real-world scenarios where new or rare object classes may emerge, allowing for more flexible and robust segmentation capabilities.

2.2 History

The origins of image segmentation can be traced back to early methods developed for object boundary detection [49], which subsequently catalyzed the development of a wide array of segmentation algorithms. Owing to the inherent similarities between image and video segmentation, many of these techniques have been extended to the video domain, spurring rapid advancements in video segmentation methodologies.

Initial attempts at VSP primarily relied on simple and efficient over-segmentation techniques [13], [50]–[53]. These methods segmented continuous video into multiple regions by detecting abrupt changes in pixel intensities or by grouping pixels based on similarity. Such segmentation provided a rudimentary partitioning of the video for subsequent post-processing. However, despite their ability to delineate regions of interest to some extent, these approaches lacked an effective mechanism for modeling the spatiotemporal information inherent in videos, making it difficult to directly produce accurate and consistent segmentation masks.

As machine learning and computer vision technologies advanced, researchers began to recognize the limitations of relying solely on low-level pixel features. This recognition led to a growing demand for high-level semantic cues and an understanding of spatiotemporal correlations to enhance parsing quality. Consequently, some scholars started incorporating sophisticated methods, such as optical flow techniques [54]–[57], graph models [13], [58], and graph cut-based methods [59] into the video segmentation process. These innovations aimed to harness motion information between consecutive frames to improve temporal stability and boundary consistency in the segmentation results.

The transformative success of deep CNNs in image segmentation [1], [18]–[20] fueled significant interest in extending these approaches to VSP. Early methods often involved a “frame-wise parsing followed by post-processing” strategy, where a trained image segmentation network parsed each individual frame. Subsequently, techniques like optical flow [60] or conditional random fields (CRF) [61] were applied to smooth the segmentation results across frames, addressing some of the temporal coherency issues encountered in earlier methods.

In recent years, the field of VSP has witnessed significant advancements, propelled by a range of innovative methodologies. Instance segmentation techniques have been successfully extended into the video domain [62], enabling more precise object-level understanding across frames. To alleviate reliance on large-scale annotated datasets, unsupervised and self-supervised learning strategies have emerged as powerful alternatives [63]–[65], effectively leveraging unlabeled data to enhance representation learning, thus addressing one of the significant bottlenecks in the field. Moreover, in the pursuit of achieving real-time performance, researchers have developed efficient architectures to strike a balance between accuracy and computational cost [24], [66]–[69]. The incorporation of Transformer-based models [70], [71] has further enhanced the ability to capture long-range temporal dependencies, enabling models to better comprehend complex scene dynamics. Additionally, advancements in dynamic network designs, predictive feature learning mechanisms, and spatiotemporal memory networks have significantly improved the ability of models to handle temporal variations in complex video scenes.

Overall, although traditional VSP methods have achieved commendable results in specific contexts, they remain constrained by the intricacies of handcrafted feature engineering. The advent

of deep learning techniques in recent years has ushered VSP into a new era, significantly enhancing its performance in complex environments. In the following sections, we provide a comprehensive introduction to the recent advancements in this domain.

2.3 Related Research Areas

Several research areas are closely related to VSP. Below is an overview of these closely related topics of VSP.

Image Semantic Segmentation. The success of image semantic segmentation [25], [72]–[76] has significantly accelerated the rapid development of the VSP field. Early VSS approaches [77], [78] primarily relied on applying image semantic segmentation methods to individual frames. However, more recent methods have systematically explored spatiotemporal consistency to improve both accuracy and efficiency. Despite these advances, image semantic segmentation remains a fundamental cornerstone for state-of-the-art VSS techniques.

Video Object Segmentation. Advancements in Video Object Segmentation (VOS), exemplified by seminal works such as [79]–[83], have significantly influenced VSP. These studies demonstrated that fine-tuning deep networks with minimal supervision and integrating spatiotemporal memory mechanisms can achieve robust, temporally consistent segmentation. Many methodologies developed in VOS have been directly adopted in VSP to enhance semantic coherence across frames, addressing complex challenges such as occlusions and rapid motion in dynamic scenes.

Video Object Detection. To extend object detection into the video domain, video object detectors have incorporated temporal cues into their conventional frameworks [84]–[89]. Both video object detection and instance-level video segmentation share core technical challenges, including the maintenance of temporal consistency, mitigation of motion blur, and handling of occlusions. By leveraging advanced temporal modeling techniques, these approaches effectively detect and segment objects in dynamic environments. Moreover, the integration of temporal information not only enhances detection accuracy but also establishes a strong foundation for VSP, where understanding scene dynamics and object interactions is essential.

3 METHODS: A SURVEY

3.1 Video Semantic Segmentation

Expanding the advancements of deep learning in image semantic segmentation into video analysis has emerged as a prominent research focus in computer vision [114]. While the most straightforward approach involves applying image segmentation models to each video frame individually, this strategy neglects the temporal continuity and coherence inherent in video data. To address this limitation, research has evolved in four key directions, each interlinked and often overlapping in methodology.

Flow-based Methods. Optical flow is a fundamental technique used to capture the apparent motion of objects across consecutive video frames, resulting from the relative motion between the camera and the observed scene [23]. Rooted in the assumption of brightness consistency, optical flow posits that the intensity of a pixel remains unchanged over time, such that any displacement in pixel position directly correlates with motion. By estimating flow vectors for each pixel, optical flow methods generate a

dense motion field that encodes the temporal relationships between frames, thereby enabling enhanced modeling of dynamic phenomena. These techniques have found widespread application in diverse video analysis tasks, including object tracking, scene flow estimation, and video segmentation, where they effectively capture the spatiotemporal dependencies that characterize motion. A key strength of optical flow-based approaches lies in their ability to preserve temporal coherence across video sequences, ensuring stable and accurate segmentation even in highly dynamic scenes.

By leveraging the dense motion field generated by optical flow, advanced models propagate temporal information and refine spatial features across frames, achieving robust segmentation under diverse conditions. One prominent strategy is the use of feature propagation, where approaches like NetWarp [3] employ optical flow to guide feature alignment across consecutive frames, ensuring temporal consistency. Similar to this idea, predictive frameworks such as PEARL [60] combine optical flow with feature prediction to further improve segmentation accuracy by capturing future motion trends. Adaptive feature propagation has also been explored through architectures like the Dynamic Video Segmentation Network (DVSNet) [68], which incorporates dynamic update mechanisms for efficient segmentation.

Moreover, the use of advanced techniques to explicitly model spatiotemporal dependencies has led to significant improvements in segmentation robustness. Methods such as GCRF [90] leverage deep spatiotemporal conditional random fields, optimizing consistency through probabilistic pixel-level interactions. Recurrent architectures like STGRU [95] introduce gating mechanisms to selectively propagate optical flow information, allowing for adaptive handling of occlusions and non-linear motion. Efficiency-focused approaches such as Accel [4] balance speed and accuracy by integrating low-resolution motion prediction with high-resolution corrections, offering a scalable solution for real-time applications. Meanwhile, joint learning frameworks like EFC [97] simultaneously optimize optical flow and segmentation tasks using bidirectional propagation, significantly improving temporal coherence. Finally, efficient temporal consistency frameworks, exemplified by ETC [100], balance computational efficiency and segmentation quality through frame-wise inference and feature-level temporal aggregation. Together, these methods highlight the versatility and effectiveness of optical flow in addressing the intricate spatiotemporal challenges of VSS, pushing the boundaries of accuracy, efficiency, and robustness in dynamic video analysis.

Attention-based Methods. Attention mechanisms have recently emerged as a popular approach in VSS, enabling models to prioritize critical spatial and temporal features dynamically. By assigning varying weights to different regions of the input, attention models selectively focus on the most relevant information, enhancing segmentation accuracy in complex and dynamic scenes [107]. Spatial attention mechanisms highlight important regions within individual frames, while temporal attention captures key moments across the video sequence. When combined with optical flow, attention mechanisms refine motion cues and improve the handling of occlusions, leading to more precise and temporally consistent segmentation. This synergy has proven effective in addressing the challenges posed by dynamic video data, offering a powerful tool for robust and adaptive segmentation.

Furthermore, it enables models to focus on the most relevant spatiotemporal features selectively and thereby improves segmentation accuracy and efficiency. By leveraging both spatial and

TABLE 1
Summary of essential characteristics for reviewed VSS methods.

Methods	Publication	Core Architectures	Technical Features	Training Datasets
VideoGCRF [90]	CVPR'2018	FCN+CRF	Gaussian CRF	DAVIS [91], [92]/CamVid [93]
EUVS [23]	ECCV'2018	Bayesian CNN	Flow-guided Feature Aggregation	CamVid [93]
LVS [69]	CVPR'2018	FCN	Keyframe Selection	CamVid [93]/Cityscapes [94]
GRFP [95]	CVPR'2018	FCN + GRU	Temporal Feature Aggregation	CamVid [93]/Cityscapes [94]
DVSNet [68]	CVPR'2018	FCN+RL	Keyframe Selection	Cityscapes [94]
Accel [4]	CVPR'2019	FCN	Keyframe Selection	KITTI [96]
SSeg [22]	CVPR'2019	FCN	Weakly-Supervised Learning	CamVid [93]/Cityscapes [94]
Naive-Student [63]	ECCV'2020	FCN+KD	Semi-Supervised Learning	Cityscapes [94]
EFC [97]	AAAI'2020	FCN	Temporal Feature Aggregation	CamVid [93]/Cityscapes [94]
TDNet [98]	CVPR'2020	Memory Network	Attention-based Feature Aggregation	CamVid [93]/Cityscapes [94]/NYUDv2 [99]
ETC [100]	ECCV'2020	FCN + KD	Knowledge Distillation	CamVid [93]/Cityscapes [94]
SDE [64]	CVPR'2021	FCN	Semi-Supervised Learning	Cityscapes [94]
CFFM [70]	CVPR'2022	Transformer	Static and motional context learning	Cityscapes [94]/VSPW [101]
MRCFA [71]	ECCV'2022	Transformer	Attention to cross-frame affinities	Cityscapes [94]/VSPW [101]
CIRKD [102]	CVPR'2022	KD	Cross-image relation	CamVid [93]/Cityscapes [94]/Pascal VOC [103]
IFR [104]	CVPR'2022	FCN	Semi-Supervised Learning	CamVid [93]/Cityscapes [94]
MVNet [105]	CVPR'2023	Transformer	Multispectral input	MVSeg [105]
SSLTM [65]	CVPR'2023	FCN + Transformer	Semi-Supervised Learning	Cityscapes [94]/VSPW [101]
MPVSS [106]	NIPS'2023	FCN + Transformer	Keyframe Selection	Cityscapes [94]/VSPW [101]
BLO [107]	CVPR'2023	Transformer	Keyframe Selection	Cityscapes [94]/ADE20K [108]/Pascal VOC [103]
VPSeg [109]	CVPR'2024	Transformer	Vanishing point	ACDC [110]/Cityscapes [94]
TDC [111]	CVPR'2024	FCN	Semi-Supervised Learning	CamVid [93]/Cityscapes [94]
CFFM+ [112]	PAMI'2024	Transformer	Global temporal contexts learning	CamVid [93]/Cityscapes [94]
TV3S [113]	CVPR'2025	Transformer + Mamba	State space	VSPW [101]/Cityscapes [94]

temporal dependencies, these mechanisms address the challenges posed by dynamic and cluttered video scenes. For instance, TDNet [98] introduces a time-distributed network architecture that combines feature distillation and multi-scale temporal aggregation, significantly enhancing segmentation speed and precision through a lightweight temporal branch. Building upon this, CFFM [70] employs a feature pyramid for adaptive, multi-scale feature fusion, while CFFM++ [112] further refines this approach with a global temporal context extraction mechanism, optimizing both segmentation accuracy and computational efficiency. Similarly, MRCFA [71] utilizes cross-frame feature correlation analysis to capture complex temporal dependencies, improving the model's ability to handle intricate motion patterns.

In parallel, CIRKD [102] leverages knowledge distillation to transfer temporal information from low-resolution features to high-resolution ones, optimizing the utilization of temporal cues. MVNet [105] adopts a multi-view feature fusion approach, enabling precise segmentation across multiple perspectives, while SSLTM [65] introduces a spatiotemporal context modeling module to model short- and long-term temporal dependencies jointly. Furthermore, MPVSS [106] employs an adaptive mask propagation strategy to balance accuracy and efficiency by utilizing keyframe segmentation results to guide non-keyframe segmentation. Finally, VPSeg [109] enhances segmentation by incorporating vanishing point (VP) priors, using both sparse-to-dense feature mining and VP-guided motion fusion to handle dynamic and static motion contexts. Collectively, these attention-based methods demonstrate the power of selectively focusing on relevant spatiotemporal features, offering robust solutions for video segmentation tasks in complex, dynamic environments.

Real-time Methods. Real-time optimization methods have emerged as a critical focus in VSS, addressing the need for high-speed processing in latency-sensitive applications without compromising accuracy. These methods achieve efficiency through lightweight architectures, adaptive scheduling, and feature reuse. For instance, Clockwork [66] employs stage-wise clock signals to selectively control computation in a fully convolutional network,

using cached results to avoid redundant processing. Similarly, LVS [69] integrates feature propagation modules with adaptive schedulers, ensuring low-latency segmentation.

Building on this foundation, dynamic methods such as DVS-Net [68] excel in optimizing resource allocation and synchronizing segmentation with optical flow networks, thereby accelerating processing while maintaining accuracy. In contrast, attention-based approaches like TDNet [98], ETC [100], CFFM [70], and MPVSS [106] enhance efficiency and real-time performance by employing innovative techniques focused on low-resolution feature management and mask propagation. TV3S [113] takes a distinctive approach by employing the Mamba state space model to independently process spatial patches, integrating a selective gating mechanism, shift operations, and a hierarchical structure. This design enables TV3S to balance accuracy and efficiency, delivering robust performance in VSS tasks. These innovations collectively demonstrate how real-time optimization in VSS can seamlessly integrate efficiency and precision, enabling robust segmentation for dynamic, resource-constrained environments.

Semi-/Weakly-supervised Methods. Semi-supervised and weakly-supervised methods have become pivotal in VSS, offering practical solutions to reduce dependence on extensively labeled datasets while ensuring high segmentation accuracy. By leveraging unlabeled or sparsely labeled video data, these methods utilize temporal coherence and spatiotemporal correlations to extract meaningful supervision signals [22], [104], [111]. A representative example is Naive-Student [63], which introduces an iterative semi-supervised learning strategy where pseudo-labels are generated for unlabeled data and refined with annotated data, bypassing the need for complex label propagation architectures.

Building on this foundation, DepthMix [64] innovatively incorporates unlabeled data into training by leveraging depth mixing techniques, combining depth supervision and distillation to maximize the utility of unlabeled samples. Additionally, SSLTM [65] utilizes an attention-based mechanism to effectively model complex spatiotemporal relationships, enhancing the integration of unlabeled data into the learning process and improving seg-

TABLE 2
Summary of essential characteristics for reviewed VIS methods.

Methods	Publication	Core Architectures	Technical Features	Training Datasets
MaskTrack R-CNN [62]	ICCV'2019	Mask R-CNN	Tracking by Detection	YouTube-VIS [62]
STEm-Seg [115]	ECCV'2020	FCN	Spatio-Temporal Embedding	DAVIS [92]/YouTube-VIS [62]/KITTI-MOTS [38]
MaskProp [116]	CVPR'2020	Mask R-CNN	Instance Feature Propagation	YouTube-VIS [62]
MVAE [117]	CVPR'2020	Mask R-CNN+VAE	Variational Inference	YouTube-VIS [62]/KITTI-MOTS [38]
MOTNet [118]	CVPR'2020	Mask R-CNN	Unsupervised Learning	KITTI-MOTS [38]/BDD100K [119]
SemiTrack [120]	CVPR'2021	SOLO	Semi-Supervised Learning	Cityscapes [94]/YouTube-VIS [62]
CompFeat [121]	AAAI'2021	Mask R-CNN	Spatio-Temporal Feature Alignment	YouTube-VIS [62]
IFC [122]	NIPS'2021	FCN + Transformer	Inter frame communication	YouTube-VIS [62]
Propose-Reduce [123]	ICCV'2021	Mask R-CNN	Propose and Reduce	DAVIS [92]/YouTube-VIS [62]
SG-Net [124]	CVPR'2021	FCOS	Single-Stage Segmentation	YouTube-VIS [62]
fIRN [125]	CVPR'2021	Mask R-CNN	Weakly-Supervised Learning	Cityscapes [94]/YouTube-VIS [62]
VisTR [126]	CVPR'2021	Transformer	Transformer-based Segmentation	YouTube-VIS [62]
TraDeS [127]	CVPR'2021	FCN	Tracking by Detection	YouTube-VIS [62]/KITTI-MOTS [38]
CrossVIS [128]	ICCV'2021	FCN	Dynamic Convolution	YouTube-VIS [62]/OVIS [129]
TPR [130]	PAMI'2022	FCN	Temporal Pyramid Routing	YouTube-VIS [62]
VISOLO [131]	CVPR'2022	Transformer	Grid based space time aggregation	COCO [132]/YouTube-VIS [62]
MinVIS [133]	NIPS'2022	Transformer	Query based track	YouTube-VIS [62]/OVIS [129]
STC [134]	ECCV'2022	FCN	Contrastive learning	YouTube-VIS [62]/OVIS [129]
TrackFormer [135]	CVPR'2022	FCN + Transformer	Track query	MOT17 [136]/MOTS20 [38]
SeqFormer [137]	ECCV'2022	Transformer	Sequential Transformer	YouTube-VIS [62]
IDOL [138]	ECCV'2022	Transformer	Contrastive learning	YouTube-VIS [62]
TeViT [139]	CVPR'2022	Transformer	Pyramid features interaction	YouTube-VIS [62]/OVIS [129]
GenVIS [140]	CVPR'2023	Transformer	Query based training pipeline	YouTube-VIS [62]/OVIS [129]
VideoCutLER [141]	CVPR'2023	DINO + FCN	Unsupervised Learning	DAVIS [92]/YouTube-VIS [62]
CTVIS [142]	ICCV'2023	Transformer	Contrastive learning	YouTube-VIS [62]/OVIS [129]
DVIS [143]	ICCV'2023	Transformer	Decoupling strategy	YouTube-VIS [62]/OVIS [129]
OVFormer [144]	ECCV'2024	Transformer	Contrastive learning	LV-VIS [145]/YouTube-VIS [62]/OVIS [129]
OV2Seg+ [146]	IJCV'2024	Transformer	Open vocabulary learning	LVIS [147]/LV-VIS [145]/YouTube-VIS [62]. . .

mentation performance. Together, these approaches demonstrate the potential of semi- and weakly-supervised methods to balance annotation efficiency and segmentation accuracy, paving the way for scalable and robust VSS in real-world scenarios.

3.2 Video Instance Segmentation

To tackle the challenge of simultaneously detecting, segmenting, and tracking instances in videos, the VIS framework, introduced by [62], was proposed. VIS integrates these tasks to enable a unified solution for instance-level video analysis. For VIS, the research has focused on three main directions, which frequently overlap to a considerable extent.

Tracking-based Methods. Tracking-based VIS methods have seen significant advancements in recent years, leading to enhanced accuracy and temporal consistency in VIS tasks [116], [117], [121], [123], [124], [128], [130]. One notable approach is MaskTrack R-CNN [62], a two-stage object detection and instance segmentation algorithm. In the first stage, it employs a Region Proposal Network (RPN) [7] to generate object candidate boxes. The second stage utilizes three parallel branches for object classification, bounding box regression, and instance segmentation, respectively, effectively achieving precise object detection and segmentation in dynamic scenes.

Building upon the concept of multi-object tracking, Multi-Object Tracking and Segmentation (MOTS) [38] incorporates pixel-level segmentation capabilities into tracking. By generating segmentation masks for each detection box, MOTS enables the precise segmentation and tracking of individual objects, enhancing the robustness of multi-object tracking in complex environments. Besides, the TraDeS model [127] introduced a joint detection and tracking framework that leverages tracking cues to assist detection. By inferring tracking offsets through a cost volume, TraDeS improves both object detection and segmentation accuracy, facilitating better handling of occlusions and motion dynamics. The

StemSeg [115] adopts a proposal-free, single-stage framework that treats the video as a 3D spatiotemporal volume, allowing for temporally consistent instance segmentation without explicit tracking. Following a different design, IFC [122] proposes an efficient per-clip architecture that processes frames with a CNN backbone, and exchanges temporal information through a two-stage inter-frame communication encoder, followed by a lightweight decoder with class and mask heads. More recently, the STC model [134] proposed a spatiotemporal consistency framework that integrates spatiotemporal features to enhance the accuracy and consistency of VIS. By modeling temporal dependencies alongside spatial features, STC ensures better continuity across video frames, making it particularly effective in capturing dynamic and evolving motion patterns in video sequences. Collectively, these methods highlight the progression of tracking-based detection approaches, which continue to push the boundaries of precision, consistency, and efficiency in dynamic video analysis.

Semi/Weakly-supervised Methods. Semi-supervised and weakly-supervised methods have emerged as critical strategies in VIS, providing efficient solutions to mitigate the reliance on large-scale labeled datasets while maintaining high segmentation accuracy. These approaches capitalize on the availability of unlabeled or sparsely labeled video data, leveraging temporal coherence and spatiotemporal relationships to generate meaningful supervisory signals. By integrating these weak supervision cues, semi-/weakly-supervised models can effectively learn to detect, segment, and track instances across video frames, even with limited annotations. A prominent semi-supervised approach is SemiTrack [120], a one-stage method that facilitates instance tracking through training on both images and unlabeled video data. This model utilizes the inherent temporal consistency in video sequences to improve the learning process and enhance tracking performance.

In contrast, fIRN [125] presents a weakly-supervised instance segmentation method that harnesses motion and temporal consis-

TABLE 3
Summary of essential characteristics for reviewed VPS methods.

Methods	Publication	Core Architectures	Technical Features	Training Datasets
VPSNet [148]	CVPR'2020	Mask R-CNN	Spatio-Temporal Feature Alignment	VIPER-VPS [148]/Cityscapes-VPS [148]
ViP-DeepLab [149]	CVPR'2021	FCN	Depth-Aware Panoptic Segmentation	Cityscapes-VPS [148]
SiamTrack [150]	CVPR'2021	Siamese FCN	Supervised Contrastive Learning	VIPER-VPS [148]/Cityscapes-VPS [148]
PVPS [151]	ECCV'2021	FCN	Panoramic video panoptic	WOD: PVPS [151]
Video K-Net [152]	CVPR'2022	Transformer	Query based learning	KITTI [96]/Cityscapes [94]/VIPSeg [48]
ClipPanoFCN [48]	CVPR'2022	FCN	Two stages segmentation	VIPSeg [48]
TubeLink [153]	ICCV'2023	Transformer	Query based learning	VIPSeg [48]
PolyphonicFormer [154]	ECCV'2022	Transformer	Query based learning	KITTI [96]/Cityscapes-VPS [148]
ODISE [155]	CVPR'2023	UNet + Transformer	Extract feature from diffusion model	ADE20K [108]/COCO [156]

tency signals within the video to refine segmentation accuracy. By exploiting the spatiotemporal cues inherent in video data, FIRN addresses the challenge of achieving accurate instance segmentation with minimal supervision. Additionally, VideoCutLER [141] proposes a simple unsupervised VIS approach, which consists of three primary steps: first, performing unsupervised segmentation on individual frames; second, synthesizing the segmentation results into a video for training; and finally, training a video segmentation model on the synthesized data. This method offers a novel pathway for unsupervised learning, making it particularly useful when labeled data is scarce or unavailable. Furthermore, MOTSNet [118] introduces an innovative pipeline for automatic training data generation, simultaneously improving the existing MOTS methods. By automating the generation of training data, MOTSNet significantly reduces the need for manual annotation, thereby enabling the development of more efficient and scalable models. This contribution enhances the ability of MOTS to handle complex multi-object scenarios, offering improved performance in dynamic environments. Collectively, these methods showcase the increasing reliance on weak and semi-supervised learning paradigms, pushing the boundaries of VIS by achieving robust performance with limited supervision.

Attention-based Methods. In recent years, attention-based architectures have redefined the landscape of VIS by leveraging attention mechanisms to cohesively integrate spatial and temporal cues [133], [135], [138]. VisTR [126] pioneers this paradigm by employing self-attention to aggregate features of the same instance across frames, subsequently applying a 3D convolutional head to predict mask sequences end to end. This unified formulation obviates the need for separate detection and tracking stages, yielding tightly coupled spatiotemporal representations, though at the expense of quadratic attention cost for long sequences. Building on this, VISOLO [131] introduces a grid-based representation enriched by a dual collaborative module: a memory-matching component that computes affinities between current and historical grid cells, and a temporal-aggregation unit that fuses past information to bolster frame-level classification and segmentation performance. In contrast, MinVIS posits that the learned query embeddings inherently capture temporal consistency, eliminating the necessity for explicit video-centric training. By simply linking instances via cosine similarity of queries, MinVIS [133] achieves comparable association accuracy with substantially reduced training complexity and accelerated inference.

Subsequent advances have sought to refine the balance between per-frame precision and long-range coherence. SeqFormer [137] advocates for decoupling temporal aggregation from spatial attention by employing standalone instance queries that independently interact with each frame’s features, thereby preserving

single-frame fidelity while capturing time series dynamics. TeViT [139] further enhances this strategy by constructing a multi-scale feature pyramid via a transformer backbone, randomly initialized instance queries then attending to these scales to directly predict video instances, enabling flexible cross-scale temporal modeling. Beyond architectural innovations, GenVIS [140] adopts a novel multi-clip training regime, sampling diverse video segments per iteration to more faithfully emulate real-world temporal variability and improve generalization. CTVIS [142] introduces a contrastive learning framework that aligns training and inference through long-sequence sampling, a memory bank of historical embeddings, and momentum-averaged query updates, substantially reinforcing temporal stability and association robustness. Finally, DVIS [143] demonstrates that decomposing VIS into separate detection, segmentation, and association streams can both elevate accuracy and dramatically lower resource consumption, highlighting the value of task-specific specialization within an attention-driven ecosystem. Collectively, these methods underscore the potency of attention for dynamic scene understanding, charting a course toward ever more efficient and coherent VIS in increasingly complex and diverse real-world environments.

3.3 Video Panoptic Segmentation

VPS [148] is a more comprehensive video segmentation task that integrates the characteristics of VSS and VIS. The goal of VPS is to assign a semantic label to every pixel in a video while simultaneously distinguishing and tracking foreground object instances and providing semantic annotations for background regions. Existing approaches to VPS can generally be categorized into three main directions.

Query-based Methods. Query-based VPS approaches formulate segmentation and tracking as a query interaction problem, enabling unified, end-to-end solutions without reliance on hand-crafted tracking mechanisms [150]. A prominent example, Video K-Net [152], extends the K-Net paradigm by introducing a set of learnable convolutional kernels that jointly represent semantic categories and object instances. These kernels dynamically interact with pixel-level features, allowing them to perform segmentation and implicitly maintain temporal consistency across frames. By learning such representations end-to-end, Video K-Net elegantly unifies semantic segmentation, instance segmentation, and tracking within a single framework. Building upon this query-centric perspective, Tube-Link [153] proposes a temporal linking strategy that segments videos into short clips, each processed by a Transformer to generate spatiotemporal tube masks. Cross-clip associations are then established through inter-query attention, capturing long-range dependencies without the need for external tracking networks. Complementing these, PolyphonicFormer

TABLE 4
Summary of essential characteristics for reviewed VTS methods.

Methods	Publication	Core Architectures	Technical Features	Training Datasets
Track R-CNN [38]	CVPR'2019	Mask R-CNN	Tracking by Detection	KITTI MOTS [38]/MOTChallenge [38]
PointTrack [157]	ECCV'2020	PointTrack	Tracking by points	APOLLO MOTS [157]
MaskProp [116]	CVPR'2020	Mask R-CNN	Instance Feature Propagation	YouTube-VIS [62]
ASB [158]	ICCV'2021	Assignment Space	Top k + Dynamic programming	KITTI MOTS [38]/MOTChallenge [38]
MPNTrackSeg [159]	IJCV'2022	MPN + GNN	Graph based	MOT20 [160]/KITTI [96]/HiEve [161]
MITS [162]	ICCV'2023	Transformer	Joint tracking and segmentation	Youtube-VOS [163]/DAVIS [91]
SAMTrack [164]	arXiv'2023	SAM + DeAOT	Multimodal interaction	DAVIS [91], [92]
SAM-PT [165]	arXiv'2023	SAM + PT	Tracking by points	DAVIS [91]/Youtube-VOS [163]/BDD100K [119]
DEVA [39]	ICCV'2023	SAM	Decoupled segmentation and tracking	VIPSeg [48]/YouTube-VIS [62]
SAM 2 [166]	arXiv'2024	SAM	Prompt segmentation	SA-V [166]

[154] introduces a unified query learning framework that effectively harnesses the mutual reinforcement between panoptic segmentation and depth information. By leveraging the synergistic interplay among semantic segmentation, instance delineation, and depth cues, PolyphonicFormer facilitates a more holistic and robust understanding of complex scenes. Collectively, these methods exemplify the versatility and strength of query-based representations in addressing the multifaceted challenges of VPS.

Depth-aware Methods. Depth-aware methods integrate the challenges of both depth estimation and semantic instance segmentation, addressing the complex task of reconstructing 3D point clouds from 2D image sequences while simultaneously providing both semantic and instance-level labels. One prominent approach, ViP-DeepLab [149], tackles the inverse projection problem in vision by effectively leveraging monocular depth estimation to infer 3D structures, thereby enhancing VPS performance. By combining these two sub-tasks, ViP-DeepLab generates a unified framework that not only recovers spatial depth information but also assigns accurate semantic and instance labels to each 3D point in the scene. Complementing this, PolyphonicFormer [154] introduces a novel query-based learning framework, which effectively harnesses the mutual enhancement between panoptic segmentation and depth information. This approach facilitates more robust scene understanding by exploiting the synergistic relationship between semantic segmentation, instance delineation, and depth cues. Through these advancements, both methods push the boundaries of depth-aware segmentation, offering a comprehensive solution for high-fidelity video scene analysis.

Dual-branch Methods. Dual-branch methods perform panoptic segmentation by decoupling the task into two parallel branches: one dedicated to semantic segmentation for stuff classes and the other focused on instance segmentation for thing classes. The final panoptic prediction is obtained by fusing the outputs from both branches in a unified representation. Panoptic-DeepLab [151] exemplifies this architecture by extending it to the VPS setting. Specifically, it reconstructs a wide 220° field of view through the stitching of images captured from five synchronized cameras. Using known camera parameters, the method projects 2D pixels into a shared 3D space, enabling segmentation to be performed within a unified geometric context. By integrating spatial cues across multiple viewpoints, Panoptic-DeepLab achieves consistent segmentation across the scene, effectively handling complex layouts and occlusions in wide-angle video environments.

3.4 Video Tracking & Segmentation

VTS is a critical task in computer vision that combines two essential processes: identifying and tracking objects over time, and

segmenting these objects from the background. The goal of VTS is to detect and follow the movement of objects across frames while simultaneously segmenting these objects from the surrounding environment, providing precise pixel-wise annotations for both foreground and background regions. This task is pivotal in a range of applications, from autonomous driving to surveillance and action recognition. Existing approaches to VTS can generally be categorized into three main directions.

Point-based Methods. Traditional VTS methods struggle with distinguishing foreground and background features due to the limitations of convolutional receptive fields, which affects tracking accuracy. The method in [157] overcomes this by treating both the foreground and surrounding regions as 2D point clouds, learning from four data modalities—offset, color, category, and position—leading to more precise segmentation and tracking. Similarly, [165] propagates positive and negative points across video frames, refining segmentation masks through iterative interactions with the SAM model [167], discarding occluded points and adding new visible ones to maintain tracking accuracy. Lastly, [162] combines segmentation masks with bounding boxes by using Transformer layers with self-attention to pinpoint object edges, enabling precise localization and unified tracking. These methods, through their innovative use of points for feature extraction, tracking, and refinement, highlight how leveraging point-based approaches can significantly enhance MOTS performance.

Two-stage Methods. Two-stage methods in VIS first generate region proposals and then perform object classification, segmentation, and association based on these proposals. This pipeline separates object localization from refinement tasks, allowing for more precise instance-level predictions and temporal tracking. A representative example is TrackR-CNN [38], which augments a ResNet-101 backbone with 3D convolutions to model spatiotemporal features. These features are processed by a Region Proposal Network (RPN), and the model further incorporates an association head that predicts embedding vectors for matching instances across frames via Euclidean distance. Bertasius *et al.* [116] extend the Mask R-CNN framework by introducing a mask propagation branch that learns instance-specific features and temporally propagates them, enabling more accurate segmentation across time. Brasó and Leal-Taixé [159] propose a graph-based formulation where nodes and edges, representing object hypotheses and their associations, are updated through neural message passing under flow conservation constraints. Their framework classifies association edges and predicts instance masks using CNN-based embeddings. More recently, SAM-Track [164] introduces a unified tracking framework supporting both interactive and automatic modes. In interactive mode, the model leverages SAM [167] and

Grounding DINO [168] to enhance reference frame segmentation and semantics. In automatic mode, the system autonomously identifies and segments new instances, reducing identity drift and improving robustness in unconstrained scenarios.

Efficient Methods. The ASB method [158] addresses local tracking issues and the combinatorial explosion of detection space in classical global methods by formulating the problem using assignment-based optimization. It calculates the top-k best detection assignments between frames using the Hungarian-Murty algorithm and a custom cost function, which combines IoU, appearance, and distance features. Dynamic programming is then applied to find the global optimal solution efficiently. Additionally, the method jointly learns tracking and deep network parameters and improves long-distance assignment by constructing a cost matrix to recover links across multiple interrupted detections. [39] introduces DEVA, which decouples segmentation and tracking tasks. It uses task-specific image-level segmentation models for single-frame segmentation and a generic bidirectional temporal propagation model to generalize across different tasks, enabling the propagation of segmentation results across video frames.

3.5 Open-Vocabulary Video Segmentation

OVVS is a cutting-edge task in computer vision that combines semantic segmentation, temporal tracking, and language-based recognition to segment and track objects in videos using natural language prompts. This approach surpasses traditional fixed-category methods by leveraging vision-language models to generalize to novel object classes, ensuring precise pixel-level segmentation across frames while maintaining consistent tracking despite challenges like occlusion and rapid motion. With applications spanning video editing, augmented reality, and autonomous driving, current methods rely on large-scale pre-training and advanced fusion architectures, although handling diverse natural language expressions and dynamic real-world conditions remains a significant challenge. In this context, the following papers introduce some innovative frameworks that push the boundaries of OVVS and offer compelling solutions to these ongoing challenges.

OVFormer [144] addresses the domain gap between vision-language model features and instance queries through unified embedding alignment. Exploiting video-level training and semi-online inference, OVFormer harnesses temporal consistency to deliver efficient and accurate *open-vocabulary VIS*. For this task, OV2Seg+ [146] employs a universal proposal generator to detect objects without category bias, a memory-induced tracking module that refines instance features across frames for stable association, and an open-vocabulary classifier by leveraging pre-trained visual-language models. CLIP-VIS [169] proposes an encoder-decoder framework that adapts the frozen CLIP model for open-vocabulary VIS by introducing class-agnostic mask generation, temporal top-K enhanced query matching, and weighted open-vocabulary classification. Meanwhile, ODISE [155] integrates pre-trained text-to-image diffusion models with a discriminative network. Through techniques such as implicit caption generation and diffusion-based mask generation and classification, ODISE achieves comprehensive *open-vocabulary VPS*. In parallel, OV2VSS [170] presents a spatiotemporal fusion module to capture inter-frame relationships, complemented by a random frame augmentation module that enhances semantic understanding. A dedicated video-text encoding module reinforces textual information processing, culminating in effective *open-vocabulary VSS*.

4 DATASETS AND METRICS

In this section, we provide a systematic overview of the datasets §4.1 and evaluation metrics §4.2 commonly used in VSP. By analyzing these fundamental resources in depth, we aim to establish a solid foundation for subsequent methodological comparisons and assessments, while highlighting the challenges and opportunities in data acquisition and performance evaluation within the field.

4.1 Video Scene Parsing Datasets

4.1.1 VSS Datasets

In the dynamic and rapidly evolving field of VSS, the importance of robust and diverse datasets cannot be overstated. These datasets facilitate groundbreaking research and directed advancements in algorithms and applications. Below, we provide a comprehensive overview of several key datasets that have greatly influenced the VSS landscape, each offering distinct features and annotations tailored for specific research areas.

- **CamVid** [93] is the first video dataset to offer semantic labels for object categories, pioneering a critical resource for studies in autonomous driving. Captured from the perspective of a driving vehicle, this dataset provides a total of ground truth semantic labels, encompassing over 10 minutes of high-quality footage at 30Hz across five continuous videos. Semantic label images are provided at 1Hz for four of the videos, and at 15Hz for one video, resulting in a total of 701 labeled frames. The dataset is carefully partitioned into training, validation, and test sets, with frame distributions of 367, 101, and 233, respectively.
- **NYUDv2** [99] is a notable dataset for research focused on indoor scenes, comprising video sequences captured by the Microsoft Kinect camera. Designed primarily for image description research, it includes 1,449 densely annotated aligned RGB and depth images covering 464 novel scenes from three cities, as well as 407,024 unlabeled frames. Each object within the dataset is assigned both class and instance identifiers, thereby enabling a thorough examination of indoor environments and facilitating the development of advanced segmentation techniques in confined settings.
- **Cityscapes** [94] is a large and diverse dataset of stereo video sequences recorded on the streets of 50 different cities. It includes 5,000 images with high-quality pixel-level annotations and an additional 20,000 images with coarse annotations to support various methods that leverage large amounts of weakly labeled data. Cityscapes defines 30 visual classes for annotation, categorized into eight comprehensive groups: flat, construction, nature, vehicle, sky, object, human, and void.
- **KITTI** [96] started as a multimodal dataset, comprising calibrated and synchronized images, radar scans, high-precision GPS information, and IMU acceleration data, which are essential for research towards autonomous vehicles. In 2018, the dataset was updated to include semantic segmentation ground truth, aligning the data format and metrics to be consistent with those of Cityscapes [94], although the image resolution is different, set at 375×1242 . The dataset features 200 training images and 200 test images, establishing itself as a benchmark in autonomous driving and related research domains.
- **ACDC** [110] is a valuable resource for understanding performance in adverse environmental conditions. It includes 8,012 images, half of which (4,006) are evenly distributed across four common adverse conditions: fog, night, rain, and snow. Each image under these adverse conditions comes with high-quality

TABLE 5
Statistics of video segmentation datasets.

Datasets	Year	Pub.	#Videos	Train/Val/Test/Dev	Annotations	Purposes	#Classes
CamVid [93]	2009	PRL	4	(frame: 467/100/233/-)	VSS	Urban	11
NYUDv2 [99]	2012	ECCV	518	(frame: 795/654/-/-)	VSS	Indoor	40
CityScapes [94]	2016	CVPR	5,000	2,975/500/1,525	VSS	Urban	19
ACDC [110]	2021	ICCV	-	(frame: 1600/406/2000)	VSS	Urban	19
VSPW [101]	2021	CVPR	3,536	2,806/343/387/-	VSS	Generic	124
MVSeg [105]	2023	CVPR	738	452/84/202	VSS	Urban	26
YouTube-VIS [62]	2019	ICCV	3,859	2,985/421/453/-	VIS	Generic	40
KITTI MOTS [38]	2019	CVPR	21	12/9/-/-	VIS	Urban	2
MOTChallenge [38]	2019	CVPR	4	-/-/-/-	VIS	Urban	1
OVIS [129]	2021	-	901	607/140/154/-	VIS	Generic	25
BDD100K [119]	2020	ECCV	100,000	7,000/1,000/2,000/-	VSS, VIS	Driving	40 (VSS), 8 (VIS)
Cityscapes-VPS [151]	2020	CVPR	500	400/100/-/-	VPS	Urban	19
VIPER-VPS [151]	2020	CVPR	124	(frame: 134K/50K/70K/-)	VPS	Urban	23
KITTI-STEP [171]	2021	-	50	12/9/29	VPS	Urban	19
MOTChallenge-STEP [171]	2021	-	4	2/2/-/-	VPS	Urban	7
VIPSeg [48]	2022	CVPR	3536	2806/343/387	VPS	Generic	124
WOD: PVPS [151]	2022	ECCV	2860	2800/20/40	VPS	Urban	28
APOLLO MOTS [157]	2020	ECCV	-	(frame: 3.4k/2.3k/5.7k/-)	VIS	Urban	-
HiEve [161]	2023	IJCV	32	19/0/13/-	VTs	Human	14
DAVIS16 [91]	2016	CVPR	50	30/20/-/-	Object-level AVOS, SVOS	Generic	-
DAVIS17 [92]	2017	-	150	60/30/30/30	Instance-level AVOS, SVOS, IVOS	Generic	-

pixel-level panoramic annotations and a corresponding normal-condition image of the same scene. Additionally, a binary mask is provided to distinguish between clear and uncertain semantic content within the image regions. A total of 1,503 corresponding normal-condition images have panoramic annotations, bringing the total number of annotated images to 5,509.

- **VSPW [101]** marks a significant advancement as the first large-scale VSS dataset covering a multitude of diverse scenes. It includes 3,536 videos and 251,632 frames of semantic segmentation images, covering 124 semantic categories, significantly surpassing previous VSS datasets in annotation quantity. Unlike earlier datasets that primarily focused on street scenes, VSPW spans over 200 distinct video scenes, greatly enhancing the diversity of the dataset. This dataset also provides annotations at a remarkable frame rate of 15 frames per second, ensuring an extensive and densely annotated resource, with over 96% of the video data available in resolutions ranging from 720p to 4K.
- **MVSeg [105]** contributes valuable insights into multi-spectral image analysis by featuring 738 calibrated RGB and thermal video pairs along with 3,545 fine-grained pixel-level semantic annotations across 26 categories. This dataset captures a variety of challenging urban scenes during both day and night, thereby bridging critical gaps in the understanding and application of multi-spectral imaging techniques.

4.1.2 VIS Datasets

- **YouTube-VIS [62]** is extended from YouTube-VOS, featuring enhanced mask annotations. It consists of 2,883 high-resolution YouTube videos, including 2,238 training videos, 302 validation videos, and 343 test videos. The dataset features a label set of 40 object categories and offers 131k high-quality instance masks, making it a valuable resource for research in this domain.
- **KITTI MOTS [38]** offers a comprehensive dataset annotated from 21 videos in the KITTI training set. With a total of 8,008 frames across 21 scenes, it provides annotations for 26,899 cars and 11,420 pedestrians. The dataset is organized into two main subsets: the training set comprises 12 videos with 5,027 frames,

annotated with 18,831 cars, 1,509 manually annotated cars, 8,073 pedestrians, and 1,312 manually annotated pedestrians. The test set consists of 9 videos with 2,981 frames, containing 8,068 cars, 593 manually annotated cars, 3,347 pedestrians, and 647 manually annotated pedestrians.

- **MOTChallenge [38]** is derived by selecting annotations from 4 out of the 7 videos in the MOTChallenge 2017 dataset. This dataset consists of 2,862 frames annotated with 26,894 pedestrians, out of which 3,930 are manually annotated, presenting a robust benchmark to evaluate tracking algorithms.
- **OVIS [129]** consists of 901 videos averaging 12.77 seconds in length, covering 25 distinct object categories. This dataset features 296k masks and 5,223 unique instances, thereby facilitating extensive research into occlusion handling.

4.1.3 VPS Datasets

- **Cityscapes-VPS [151]** carefully annotated frames, distributed into 2,400 frames allocated for training, 300 frames designated for validation, and 300 frames reserved for testing. Each 30-frame video sequence includes annotations for 6 frames, separated by a 5-frame interval, facilitating segmentation tasks across 19 distinct semantic classes.
- **VIPER-VPS [151]** leverages the synthetic VIPER dataset extracted from the GTA-V game engine. It includes 254K frames of driving scenes centered around the protagonist, with pixel-level semantic and instance segmentation annotations for 10 *thing* classes and 13 *stuff* classes at a resolution of 1080 × 1920.
- **KITTI-STEP [171]** consists of 50 videos, totaling 18,181 frames. It includes annotations for 2 *thing* classes and 17 *stuff* classes, with a total of 126,529 annotated masks.
- **MOTChallenge-STEP [171]** consists of 4 videos, totaling 2,075 frames. The dataset includes annotations for 1 *thing* class and 6 *stuff* classes, with a total of 17,232 annotated masks.
- **VIPSeg [48]** comprises 3,536 videos with a total of 84,750 frames. It covers 232 scenes and includes 124 categories, comprising 58 *thing* classes and 66 *stuff* classes. The dataset includes a total of 926,213 instance masks.

- **WOD: PVPS [151]** is derived from WOD with further processing of annotations, providing a dataset with consistent panoramic segmentation annotations across multiple cameras and over time. It contains a total of 2,860 videos and 100,000 frames, including 8 tracking classes and 28 semantic classes.

4.1.4 VTS Datasets

- **APOLLO MOTS [157]** is built on the ApolloScape dataset, which contains 22,480 frames with VIS labels. Focused on cars due to the lower number of pedestrians, it provides a challenging MOTs dataset for both 2D and 3D tracking. The dataset is split into training, validation, and testing sets (30%, 20%, 50%), ensuring consistent tracking difficulty. APOLLO MOTs features twice as many tracks and car annotations as KITTI MOTs, with an average car density of 5.65 cars per frame, much higher than KITTI MOTs. It also contains 2.5 times more crowded cars, making tracking more complex.
- **HiEve [161]** is a large-scale dataset designed for human-centric video analysis in complex events. It offers comprehensive annotations for human motions, poses, and actions, with a focus on crowds and complex scenarios. The dataset includes over 1 million pose annotations, more than 56,000 action instances in complex events, and one of the largest collections of long-duration trajectories, averaging over 480 frames per trajectory.
- **DAVIS16 [91]** consists of 50 sequences in total, split into 30 training and 20 validation sequences. The total number of frames across all sequences is 3455, with an average of 69.1 frames per sequence. Each sequence contains one object on average, and the dataset covers 50 objects across all sequences.
- **DAVIS17 [92]** features a larger, more complex dataset with 150 sequences, 10,459 annotated frames, and 376 objects. It includes multiple objects per scene, with increased complexity due to more distractors, smaller objects, occlusions, and fast motion.

The detailed information of the datasets used in this study is systematically summarized and presented in Tab. 5.

4.2 Metrics

In this chapter, we present a comprehensive review of several widely adopted metrics alongside their corresponding computational methodologies. Through a rigorous examination of both their theoretical foundations and practical implementations, we aim to establish a robust framework that not only enhances our understanding but also underpins the subsequent analyses.

Intersection over Union (IoU). IoU, also referred to as the Jaccard Index, is a fundamental metric used to evaluate segmentation performance. It quantifies the degree of overlap between the predicted segmentation mask and the corresponding ground truth. The IoU is mathematically defined as:

$$\text{IoU} = \frac{\text{TP}}{\text{TP} + \text{FP} + \text{FN}}, \quad (1)$$

where TP, FP, and FN are the true positives, false positives, and false negatives, respectively. An IoU value closer to one reflects a greater overlap between the predicted mask and the ground truth, indicating improved segmentation accuracy. This metric is particularly valuable as it penalizes both over-segmentation and under-segmentation errors, thereby providing a comprehensive evaluation of model performance.

Mean Intersection over Union (mIoU). The metric mIoU is a popular extension of IoU that calculates the average IoU across all C classes:

$$\text{mIoU} = \frac{1}{C} \sum_{i=1}^C \text{IoU}_i. \quad (2)$$

A higher mIoU indicates improved accuracy and consistency of overlaps with the ground truth across all classes. By averaging class-wise IoU metrics, mIoU effectively balances performance among different categories, providing a holistic measure of segmentation quality that is essential for multi-class evaluations.

Video Consistency (VC). VC assesses the temporal consistency of segmentation models across consecutive frames. Let C denote the total number of frames in a video and n be the number of consecutive frames considered for consistency evaluation. The ground truth for the i -th frame is represented as S_i and the predicted label as S'_i . The VC metric over n consecutive frames, denoted as VC_n , is calculated as follows:

$$\text{VC}_n = \frac{1}{C - n + 1} \sum_{i=1}^{C-n+1} \frac{(\bigcap_{j=0}^{n-1} S_{i+j}) \cap (\bigcap_{j=0}^{n-1} S'_{i+j})}{\bigcap_{j=0}^{n-1} S_{i+j}} \quad (3)$$

To derive a comprehensive metric, the mean VC (mVC_n) across all videos in the dataset can be computed as:

$$\text{mVC}_n = \frac{1}{N} \sum_{k=1}^N \text{VC}_n^{(k)}, \quad (4)$$

where $\text{VC}_n^{(k)}$ is the VC_n value for the k -th video and N is the total number of videos analyzed. A higher VC_n (and thus mVC_n) indicates stronger temporal consistency in the segmentation predictions across consecutive frames, reflecting a model's ability to maintain coherent semantic labels over time.

Frames per Second (FPS). FPS is another critical performance indicator that defines the processing rate of frames. It is derived as follows:

$$\text{costTime} = \frac{1}{N} \sum_{i=1}^N t_i, \quad (5)$$

where t_i denotes the time to process the i -th frame, and N is the total number of frames measured. The FPS is given by:

$$\text{FPS} = \frac{1}{\text{costTime}}. \quad (6)$$

A higher FPS value indicates faster overall performance, as more frames can be processed per second, which is vital for applications requiring real-time performance.

Max Latency. Max Latency captures the worst-case processing time by identifying the slowest frame in the sequence:

$$\text{Max Latency} = \max_{1 \leq i \leq N} \{t_i\}. \quad (7)$$

This metric is especially relevant for real-time applications where even a single large delay can impact the overall user experience.

Average Precision (AP). AP extends the image-based AP metric into the temporal dimension, providing a comprehensive measure for video evaluations. The AP for video is mathematically defined as:

$$\text{AP} = \frac{1}{|T|} \sum_{t \in T} \text{AP}_t, \quad (8)$$

where AP_t denotes the average precision at a specific IoU threshold t , and $|T|$ represents the total number of IoU thresholds considered.

Average Recall (AR). AR measures the maximum recall rate achievable when a fixed number of segmented instances are provided per video. It is defined as:

$$AR = \frac{1}{|V|} \sum_{v \in V} \frac{TP_v(K)}{GT_v}, \quad (9)$$

where $TP_v(K)$ denotes the number of true positive predictions among the top K segmented instances for video v , GT_v represents the total number of ground truth segments in that video, and $|V|$ is the total number of videos evaluated. A higher AR value signifies that the model effectively captures a larger proportion of the true instances, even when the prediction scope is limited.

Segmentation and Tracking Quality (STQ) : STQ synthesizes two sub-metrics: Association Quality (AQ) and Segmentation Quality (SQ). The Association Quality is defined as:

$$AQ = \frac{1}{|G|} \sum_{z_g \in G} \frac{1}{|gid(z_g)|} \sum_{\substack{z_f \\ |z_f \cap z_g| \neq \emptyset}} TPA(z_f, z_g) \times \text{IoU}_{id}(z_f, z_g), \quad (10)$$

where G represents the set of ground truth instances, $gid(z_g)$ denotes the set of predicted instances associated with the ground truth instance z_g , $TPA(z_f, z_g)$ measures the true positive association between a predicted instance z_f and z_g , and $\text{IoU}_{id}(z_f, z_g)$ is the identity-aware IoU. The Segmentation Quality is given by:

$$SQ = \frac{1}{|C|} \sum_{c \in C} \frac{|f_{\text{sem}}(c) \cap g_{\text{sem}}(c)|}{|f_{\text{sem}}(c) \cup g_{\text{sem}}(c)|}, \quad (11)$$

where C denotes the set of classes, and $f_{\text{sem}}(c)$ and $g_{\text{sem}}(c)$ are the predicted and ground truth segmentation masks for class c , respectively. Finally, STQ is obtained by combining AQ and SQ as:

$$STQ = \sqrt{AQ \times SQ}, \quad (12)$$

thus integrating both association and segmentation performance into a singular evaluation metric. This metric provides valuable insights into the efficacy of models in VIS challenges.

Multi-Object Tracking and Segmentation Precision (MOTSP) It quantifies the precision of segmentation masks within a multi-object tracking context. It is computed as:

$$\text{MOTSP} = \frac{\sum_t \sum_{(i,j) \in \mathcal{M}_t} \text{IoU}(i, j)}{\sum_t |\mathcal{M}_t|}, \quad (13)$$

where \mathcal{M}_t denotes the set of matched pairs between predicted and ground truth masks in frame t , and $\text{IoU}(i, j)$ is the IoU between the i -th predicted mask and the j -th ground truth mask. A higher MOTSP value indicates greater overall segmentation precision in the multi-object tracking scenario.

Identity Switches (IDS). IDS measures the consistency of identity assignment in multi-object tracking and segmentation. It quantifies the number of times a ground truth object is matched to a predicted mask with a different identity than in the previous frame. Specifically, for a ground truth mask $m \in M$, if it is matched in the current frame and also has a matched predecessor mask in the previous frame (i.e., $\text{pred}(m) \neq \emptyset$), and if the identity

of these two matched predictions differs, then it is counted as an identity switch. Formally, IDS is defined as:

$$IDS = \{m \in M \mid c^{-1}(m) \neq \emptyset \wedge \text{pred}(m) \neq \emptyset \wedge id_{c^{-1}(m)} \neq id_{c^{-1}(\text{pred}(m))}\}. \quad (14)$$

Here, $c^{-1}(m)$ denotes the predicted mask matched to the ground truth mask m ; $\text{pred}(m)$ is the matched predecessor of m from previous frames; and $id_{c^{-1}(m)}$, $id_{c^{-1}(\text{pred}(m))}$ represent the tracking IDs of the matched predicted masks in the current and predecessor frames, respectively. A lower IDS value indicates more stable and consistent identity tracking performance.

Multi-Object Tracking and Segmentation Accuracy (MOTSA). It assesses the overall accuracy of tracking and segmentation, taking into account correct matches, erroneous detections, and identity (ID) switches. It is defined as:

$$\text{MOTSA} = \frac{\sum_t (|TP_t| - |FP_t| - |IDS_t|)}{\sum_t |GT_t|}, \quad (15)$$

where TP_t denotes the number of true positives (correct matches) in frame t ; FP_t represents the false positives (erroneous detections) in frame t ; IDS_t indicates the number of ID switches in frame t ; and GT_t is the total number of ground truth objects in frame t .

Soft Multi-Object Tracking and Segmentation Accuracy (sMOTSA). The metric sMOTSA is a softened version of MOTSA that incorporates IoU values to weight true positives, thereby providing a more refined assessment of segmentation quality. It is defined as:

$$\text{sMOTSA} = \frac{\sum_t \left(\sum_{(i,j) \in \mathcal{M}_t} \text{IoU}(i, j) - |FP_t| - |IDS_t| \right)}{\sum_t |GT_t|}, \quad (16)$$

where \mathcal{M}_t denotes the set of matched pairs between predicted and ground truth masks in frame t ; $\text{IoU}(i, j)$ represents the IoU of the matched pair (i, j) ; FP_t is the number of false positives in frame t ; IDS_t indicates the number of ID switches in frame t ; and GT_t is the total number of ground-truth objects in frame t . This weighting mechanism enables the sMOTSA metric to more accurately reflect the quality of the segmentation results.

Video Panoptic Quality (VPQ). It extends the concept of panoptic quality into the video domain by jointly evaluating segmentation and tracking performance across video segments. The computation process involves three steps. First, a video segment is selected. Next, for each video segment, the IoU is calculated for every pair of ground truth and predicted trajectories. True positives (TP), false positives (FP), and false negatives (FN) are determined based on a predefined IoU threshold (where TP is defined for matches with $\text{IoU} > 0.5$, FP for predictions without corresponding ground truth, and FN for ground truths that are missed by predictions). Finally, VPQ is defined as:

$$\text{VPQ}_k = \frac{1}{N_{\text{classes}}} \sum_c \frac{\sum_{(u, \hat{u}) \in T_P^c} \text{IoU}(u, \hat{u})}{|T_P^c| + \frac{1}{2}|F_P^c| + \frac{1}{2}|F_N^c|}, \quad (17)$$

where N_{classes} denotes the total number of classes, T_P^c is the set of true positives for class c , F_P^c represents the false positives, and F_N^c indicates the false negatives for class c . Notably, when $k = 0$, VPQ reduces to the standard Panoptic Quality (PQ).

TABLE 6
Quantitative VSS results on the Cityscapes val set [94] in terms of $mIoU_{class}$ and FPS.

Methods	Backbones	mIoU	FPS
DVSNet [68]	ResNet-101	70.4	19.8
LVS [69]	ResNet-101	76.8	5.8
GRFP(5) [95]	ResNet-101	69.4	3.3
Accel [4]	ResNet-101	75.5	1.1
TDNet [98]	ResNet-50	79.9	5.6
ETC [100]	ResNet-18	73.1	9.5
Lukas [64]	ResNet-101	71.2	1.9
CIRKD [102]	ResNet-18	74.7	-
MRCFA [71]	MiT-B1	75.1	21.5
CFFM [70]	MiT-B1	75.1	23.6
MPVSS [106]	Swin-L	81.6	7.2
BLO [107]	Searched	74.7	30.8
SSLTM [65]	ResNet-50	79.7	-
VPSeg [109]	MiT-B3	82.5	-
CFFM+ [112]	MiT-B1	78.7	20.4
TV3S [113]	MIT-B1	75.6	-

5 PERFORMANCE COMPARISON

In this section, we present a comprehensive performance comparison of the previously discussed VSP methods, with the results succinctly summarized in a table. For clarity and brevity, we focus exclusively on those approaches—namely VSS, VIS, and VPS—that are underpinned by rigorous and standardized performance evaluations.

5.1 VSS Benchmark

5.1.1 Evaluation Metrics

The mIoU metric is the most widely adopted evaluation metric for VSS. Among existing benchmarks, Cityscapes [94] remains the most commonly utilized dataset for VSS. It comprises 19 classes grouped into 8 high-level categories, where categories denote broader semantic concepts (*e.g.*, vehicles), and classes refer to more fine-grained distinctions (*e.g.*, bicycle, car). In our evaluation, we use per-class IoU ($mIoU_{class}$, hereafter referred to as IoU) to assess segmentation accuracy, while FPS and maximum latency are employed to measure inference efficiency.

5.1.2 Results

Tab. 6 summarizes the results of sixteen VSS approaches on Cityscapes [94] val set. VPSeg [109] achieves the highest segmentation accuracy with an mIoU of 82.5, while BLO [107] obtains the best inference speed with 30.8 FPS. Moreover, we conducted experiments on the VSPW [101] dataset using several representative VSS methods; the experimental results are summarized in Tab. 7. TubeFormer [172] achieves the best performance on all mIoU (63.2) and mVC₈ (92.1). TV3S achieves the best performance on mVC₈.

5.2 VIS Benchmark

5.2.1 Evaluation Metrics

For VIS performance evaluation, precision and recall metrics are mostly employed. Specifically, we use the metrics mentioned in [62], which are average precision (AP) and average recall (AR) based on a spatiotemporal IoU metric. CTVIS [142] achieves the best performance in terms of AP50 (78.2), AP75 (59.1), AR1 (51.9), AR10 (63.2), and overall AP (55.1), setting the new state-of-the-art on the YouTube-VIS validation set.

TABLE 7
Benchmark results for VSS on the VSPW validation dataset [101]. The results are with mIoU and mVC metrics. Methods in gray use open-vocabulary supervision.

Methods	Backbones	mIoU	mVC ₈	mVC ₁₆
CFFM [70]	MiT-B5	49.3	90.8	87.1
CFFM+ [112]	MiT-B5	50.1	90.8	87.4
MRCFA [71]	MiT-B5	49.9	90.9	87.4
TCB [101]	ResNet-101	37.5	87.0	82.1
Video K-Net [152]	ResNet-101	38.0	87.2	82.3
MPVSS [106]	ResNet-101	38.8	84.8	79.6
TV3S [113]	MiT-B5	49.8	91.7	88.7
TubeFormer [172]	Axial-ResNet	63.2	92.1	87.9
OV2VSS [170]	ResNet-101	17.22	-	-

TABLE 8
Evaluation of VIS methods on the YouTube-VIS validation set [62] in terms of AP and AR metrics. Methods in gray use open-vocabulary supervision.

Methods	Backbones	AP50	AP75	AR1	AR10	AP
MaskTrack R-CNN [62]	ResNet-50	51.1	32.6	31.0	35.5	30.3
STEm-Seg [115]	ResNet-50	50.7	33.5	31.6	37.1	30.6
fIRN [125]	ResNet-50	27.2	6.2	12.3	13.6	10.5
CrossVIS [128]	ResNet-50	56.8	38.9	35.6	40.7	39.8
SemiTrack [120]	ResNet-50	61.1	39.8	36.9	44.5	38.3
MaskProp [116]	STSN-ResNeXt-101-64x4d	-	51.2	44.0	52.6	46.6
CompFeat [121]	ResNet-50	56.0	38.6	33.1	40.3	35.3
TraDeS [127]	DLA-34	52.6	32.8	30.1	29.1	31.6
SG-Net [124]	ResNet-50	56.1	36.8	35.8	40.8	34.8
VisTR [126]	ResNet-50	59.8	36.9	37.2	42.4	36.2
Propose-Reduce [123]	ResNet-50	63.0	43.8	41.1	49.7	40.4
TeVIT [139]	MsgShiT	71.3	51.6	44.9	54.3	46.6
VISOLO [131]	ResNet-50	56.3	43.7	35.7	42.5	38.6
SeqFormer [137]	ResNet-50	69.8	51.8	45.5	54.8	47.4
IDOL [138]	ResNet-50	74.0	52.9	47.7	58.7	49.5
STC [134]	ResNet-50	57.2	38.6	36.9	44.5	36.7
MinVIS [133]	ResNet-50	69.0	52.1	45.7	55.7	47.4
GenVIS [140]	ResNet-50	72.0	57.8	49.5	60.0	51.3
VideoCutLER [141]	ResNet-50	50.7	24.2	-	42.4	26.0
DVIS [143]	ResNet-50	76.5	58.2	47.4	60.4	52.6
CTVIS [142]	ResNet-50	78.2	59.1	51.9	63.2	55.1
OV2Seg+ [146]	ResNet-50	-	-	-	-	32.9
OVFormer [144]	ResNet-50	-	-	-	-	34.8
CLIP-VIS [169]	ResNet-50	-	-	-	-	32.2

5.2.2 Results

Tab. 8 summarizes the results of twenty-one VIS approaches on YouTube-VIS-2019 [62] val set.

5.3 VPS Benchmark

5.3.1 Evaluation Metrics

For VPS tasks, the most commonly employed metrics are VPS and STQ. We have compiled the performance of mainstream VPS models on three leading datasets—Cityscapes-VPS, KITTI-STEP, and VIPSeg.

5.3.2 Results

Tab. 9 summarizes the results of nine VIS approaches on Cityscapes-VPS, KITTI-STEP, and VIPSeg. PolyphonicFormer [154] achieves the best results on Cityscapes-VPS. Video K-Net [152] achieves the best results on the KITTI-STEP dataset. TubeLink [153] achieves the best results on the VIPSeg dataset.

TABLE 9
Benchmark results on VPS validation datasets. The results are evaluated with VPQ and STQ metrics.

Methods	Backbones	Cityscapes-VPS [151] (VPQ)	KITTI-STEP [171] (STQ)	VIPSeg [48] (STQ)
VPSNet [148]	ResNet-50	57.4	-	-
VIP-Deeplab [149]	ResNet-50	63.1	-	-
SimTrack [150]	ResNet-50	57.8	-	-
Tube-PanopticFCN [48]	ResNet-50	-	-	31.5
PolyphonicFormer [154]	ResNet-50	65.4	-	-
TubeFormer [172]	Axial-ResNet	-	70.0	-
SLOT-VPS [173]	Swin-L	63.7	-	-
TubeLink [153]	Swin-B	-	72.2	49.4
Video K-Net [152]	Swin-B	62.2	73.0	46.3

TABLE 10
Evaluation of VIS methods on the KITTI-MOTS validation set [38] using sMOTSA, MOTSA, and IDS metrics.

Methods	Detectors	Cars			Pedestrians		
		sMOTSA	MOTSA	IDS	sMOTSA	MOTSA	IDS
Track R-CNN [38]	Track R-CNN	76.2	87.8	93	46.8	65.1	78
CIWT [174]	Track R-CNN	68.1	79.4	106	42.9	61.0	42
MOTSFusion [175]	Track R-CNN	78.2	90.0	36	50.1	68.0	34
CAMOT [176]	Track R-CNN	67.4	78.6	220	39.5	57.6	131
ASB [158]	Track R-CNN	77.4	89.6	41	48.9	66.7	28
PointTrack [157]	Track R-CNN	85.5	94.9	22	62.4	77.3	19

5.4 VTS Benchmark

5.4.1 Evaluation Metrics

For VTS tasks, the most commonly employed metrics are sMOTSA, MOTSA and IDS. We have compiled the performance of mainstream VTS models on the KITTI-MOTS validation set.

5.4.2 Results

Tab. 10 summarizes the results of six VIS methods on the KITTI-MOTS validation set using sMOTSA, MOTSA, and IDS for both cars and pedestrians. PointTrack [157] achieves the best results across all metrics for both object categories, with the highest sMOTSA and MOTSA scores and the lowest number of identity switches (IDS).

5.5 OVVS Benchmark

We present the results for open-vocabulary VSS in Tab. 7 and for open-vocabulary VIS in Tab. 8. As can be observed, OVVS still has a long way to go to catch up with fully supervised VSP methods. Nevertheless, its ability to segment new categories opens the door to numerous practical applications. With the continued development of large multimodal foundation models, significant improvements in OVVS accuracy are anticipated.

6 FUTURE DIRECTIONS

Open-World Video Scene Parsing. Real-world environments are inherently dynamic, unstructured, and open-ended, continuously presenting novel objects, scenes, and events that defy the constraints of any predefined semantic taxonomy. This open-world nature poses a formidable challenge to VSP systems, which traditionally rely on a closed-world assumption with a fixed set of annotated categories. Consequently, state-of-the-art VSP models, despite their impressive performance in benchmark settings, often exhibit brittle generalization, semantic rigidity, and a tendency to misclassify or ignore unseen categories when

deployed in unconstrained, real-world scenarios. To address these limitations, a growing body of research [177]–[183] has begun to tackle the open-world VSP problem, aiming to endow models with the ability to recognize known categories while simultaneously discovering, segmenting, and adapting to novel or evolving classes over time. These methods leverage a range of strategies, including open-set recognition, continual learning, prompt-based adaptation, and foundation models trained on large-scale web data. Encouragingly, these efforts are not only improving the robustness and adaptability of VSP systems but also establishing a solid foundation for building models capable of generalizing to novel categories and sustaining performance in open-world, real-world environments.

Unified Video Scene Parsing. Most video segmentation tasks face a common set of challenges, including occlusion, deformation, and the handling of long-term dependencies. Many approaches converge on similar solution frameworks to address these issues. One particularly promising research direction involves unifying multiple video segmentation tasks within a single model that operates across diverse datasets, thereby achieving robust and generalizable segmentation performance under various conditions. Recent investigations [184]–[191] have increasingly focused on the development of unified architectures, which hold significant practical value—especially in applications such as robotics and autonomous driving.

Multimodal Fusion for Segmentation. As video understanding increasingly requires precise scene decomposition, integrating heterogeneous modalities—such as RGB, depth, text, motion, and audio—has become a key strategy for enhancing segmentation accuracy and robustness. Multi-modal fusion methods leverage complementary signals to resolve ambiguous boundaries, suppress modality-specific noise, and recover fine-grained structures often missed by unimodal approaches. Recent advances span cross-modal attention and unified encoder–decoder architectures that align and aggregate features across pixel and region levels, enabling robust instance and foreground–background separation in dynamic scenes [192]–[199]. In domains such as autonomous driving, human–robot interaction, and video editing, such strategies improve semantic coherence and spatial precision. Future research should focus on scalable, modality-adaptive fusion frameworks and self-supervised objectives that promote cross-modal consistency under real-world constraints.

Visual Reasoning for Segmentation. An emerging direction in video segmentation is to integrate explicit visual reasoning, enabling models to capture temporal consistency, infer occluded objects, and interpret inter-object interactions beyond

raw pixel cues. By incorporating reasoning modules or leveraging vision–language models, segmentation systems can address challenges like occlusion, complex motion, and ambiguous boundaries through richer scene understanding. This paradigm shift supports downstream tasks such as action recognition and predictive scene parsing by grounding masks in relational context. Recent work [200]–[203] explores approaches including spatiotemporal tokens, graph-based modules, and physics-inspired predictors, aiming to bridge low-level perception with high-level video understanding.

Generative Segmentation. With the advancement of generative models, a remarkable ability to capture high-resolution features within images has emerged. Recent studies [145], [204]–[207] have begun to exploit the inherent fine-grained representations of generative models to address image segmentation challenges. By leveraging the multi-scale and high-resolution features embedded in these models, this approach not only enables a more precise recovery of local structural details in complex scenes but also offers an effective remedy for issues such as occlusion and blurred boundaries, providing a fresh perspective to conventional segmentation strategies. Currently, this direction is rapidly gaining attention as a frontier research hotspot in the field of image segmentation, with promising applications in areas such as medical image diagnosis, autonomous driving, and remote sensing analysis. It underscores the substantial potential and practical value of generative models in advancing segmentation tasks.

Efficient Video Understanding. With the surge of video data and growing demand for real-time scene analysis, efficient VSP has become a key research focus. Recent efforts [208]–[213] explore lightweight architectures, temporal fusion, and multi-scale feature extraction to enhance spatiotemporal modeling while maintaining low latency. By leveraging motion estimation and multi-frame cues, these methods better capture rapid transitions and subtle dynamics, addressing challenges like occlusion, blur, and background clutter. Efficient VSP holds promise for applications in autonomous driving, surveillance, virtual reality, and interactive media, offering a path toward scalable, real-time video understanding.

Large Language Model-based Segmentation. With the rise of large-scale pre-trained and foundation models, segmentation methods built upon these architectures have achieved significant breakthroughs. Recent works [214]–[221] exploit their rich contextual understanding and fine-grained representations to enable accurate target delineation in complex scenes. Through multi-scale feature fusion and deep semantic modeling, these methods exhibit strong robustness to occlusion and boundary ambiguity, while improving generalization in few-shot and cross-domain settings. Such approaches show great potential in domains like medical imaging, remote sensing, and autonomous driving.

7 CONCLUSION

In summary, our comprehensive survey of VSP reveals a field in dynamic evolution, characterized by rapid advancements in both methodology and application. The transition from classical techniques reliant on handcrafted features to sophisticated deep learning frameworks—integrating convolutional, attention-based, and transformer mechanisms—has substantially improved segmentation accuracy and temporal coherence in diverse scenarios. However, significant challenges persist, including effective fusion of spatiotemporal information, maintaining consistency across long

video sequences, and addressing the limitations of pre-defined label sets in open-vocabulary settings. The rapid development of new datasets and evaluation metrics has provided invaluable benchmarks, yet the gap between academic research and industrial deployment remains evident. Looking forward, future research should focus on enhancing model efficiency, robustness against complex real-world dynamics, and adaptability to unforeseen visual concepts. Our review not only consolidates current knowledge but also charts a clear path for future innovations that will drive the next generation of intelligent video analysis systems.

REFERENCES

- [1] E. Shelhamer, J. Long, and T. Darrell, “Fully convolutional networks for semantic segmentation,” *IEEE Trans. Pattern Anal. Mach. Intell.*, vol. 39, no. 4, pp. 640–651, 2017.
- [2] X. Zhu, Y. Xiong, J. Dai, L. Yuan, and Y. Wei, “Deep feature flow for video recognition,” in *IEEE Conf. Comput. Vis. Pattern Recog.*, 2017, pp. 2349–2358.
- [3] R. Gade, V. Jampani, and P. Gehler, “Semantic video CNNs through representation warping,” in *Int. Conf. Comput. Vis.*, 2017, pp. 4463–4472.
- [4] S. Jain, X. Wang, and J. E. Gonzalez, “Accel: A corrective fusion network for efficient semantic segmentation on video,” in *IEEE Conf. Comput. Vis. Pattern Recog.*, 2018, pp. 8858–8867.
- [5] A. Kundu, V. Vineet, and V. Koltun, “Feature space optimization for semantic video segmentation,” in *IEEE Conf. Comput. Vis. Pattern Recog.*, 2016, pp. 3168–3175.
- [6] S.-P. Lee, S.-C. Chen, and W.-H. Peng, “GSVNet: Guided spatially-varying convolution for fast semantic segmentation on video,” in *IEEE Int. Conf. Multimedia Expo*, 2021, pp. 1–6.
- [7] S. Ren, K. He, R. B. Girshick, and J. Sun, “Faster R-CNN: Towards real-time object detection with region proposal networks,” *IEEE Trans. Pattern Anal. Mach. Intell.*, vol. 39, no. 6, pp. 1137–1149, 2015.
- [8] S. Caelles, A. Montes, K.-K. Maninis, Y. Chen, L. Van Gool, F. Perazzi, and J. Pont-Tuset, “The 2018 DAVIS challenge on video object segmentation,” *arXiv preprint arXiv:1803.00557*, 2018.
- [9] C. Lam and M.-C. Lee, “Video segmentation using color difference histogram,” in *IAPR International Workshop on Multimedia Information Analysis and Retrieval*, 1998, pp. 159–174.
- [10] S. Fazekas, T. Amiaz, D. Chetverikov, and N. Kiryati, “Dynamic texture detection based on motion analysis,” *Int. J. Comput. Vis.*, vol. 82, pp. 48–63, 2009.
- [11] H. A. Rashwan, M. A. Mohamed, M. A. García, B. Mertsching, and D. Puig, “Illumination robust optical flow model based on histogram of oriented gradients,” in *Pattern Recogn.* Springer, 2013, pp. 354–363.
- [12] C.-P. Yu, H. M. Le, G. J. Zelinsky, and D. Samaras, “Efficient video segmentation using parametric graph partitioning,” in *Int. Conf. Comput. Vis.*, 2015, pp. 3155–3163.
- [13] M. Grundmann, V. Kwatra, M. Han, and I. Essa, “Efficient hierarchical graph-based video segmentation,” in *IEEE Conf. Comput. Vis. Pattern Recog.*, 2010, pp. 2141–2148.
- [14] F. Perazzi, O. Wang, M. H. Gross, and A. Sorkine-Hornung, “Fully connected object proposals for video segmentation,” in *Int. Conf. Comput. Vis.*, 2015, pp. 3227–3234.
- [15] V. Badrinarayanan, I. Budvytis, and R. Cipolla, “Semi-supervised video segmentation using tree structured graphical models,” in *IEEE Trans. Pattern Anal. Mach. Intell.*, vol. 35, no. 11. IEEE, 2013, pp. 2751–2764.
- [16] W.-D. Jang and C.-S. Kim, “Streaming video segmentation via short-term hierarchical segmentation and frame-by-frame markov random field optimization,” in *Eur. Conf. Comput. Vis.*, 2016, pp. 599–615.
- [17] B. Liu and X. He, “Multiclass semantic video segmentation with object-level active inference,” in *IEEE Conf. Comput. Vis. Pattern Recog.*, 2015, pp. 4286–4294.
- [18] L.-C. Chen, G. Papandreou, I. Kokkinos, K. Murphy, and A. L. Yuille, “DeepLab: Semantic image segmentation with deep convolutional nets, atrous convolution, and fully connected CRFs,” *IEEE Trans. Pattern Anal. Mach. Intell.*, vol. 40, no. 4, pp. 834–848, 2018.
- [19] H. Zhao, J. Shi, X. Qi, X. Wang, and J. Jia, “Pyramid scene parsing network,” in *IEEE Conf. Comput. Vis. Pattern Recog.*, 2017, pp. 2881–2890.

- [20] H. Ding, X. Jiang, B. Shuai, A. Q. Liu, and G. Wang, "Context contrasted feature and gated multi-scale aggregation for scene segmentation," in *IEEE Conf. Comput. Vis. Pattern Recog.*, 2018, pp. 2393–2402.
- [21] Y.-H. Tsai, M.-H. Yang, and M. J. Black, "Video segmentation via object flow," in *IEEE Conf. Comput. Vis. Pattern Recog.*, 2016, pp. 3899–3908.
- [22] Y. Zhu, K. Sapra, F. A. Reda, K. J. Shih, S. Newsam, A. Tao, and B. Catanzaro, "Improving semantic segmentation via video propagation and label relaxation," in *IEEE Conf. Comput. Vis. Pattern Recog.*, 2019, pp. 8856–8865.
- [23] P.-Y. Huang, W.-T. Hsu, C.-Y. Chiu, T.-F. Wu, and M. Sun, "Efficient uncertainty estimation for semantic segmentation in videos," in *Eur. Conf. Comput. Vis.*, 2018, pp. 520–535.
- [24] M. Paul, C. Mayer, L. V. Gool, and R. Timofte, "Efficient video semantic segmentation with labels propagation and refinement," in *IEEE Winter Conf. App. Comput. Vis.*, 2020, pp. 2873–2882.
- [25] H. Zhao, X. Qi, X. Shen, J. Shi, and J. Jia, "ICNet for real-time semantic segmentation on high-resolution images," in *Eur. Conf. Comput. Vis.*, 2018, pp. 405–420.
- [26] A. Vaswani, N. Shazeer, N. Parmar, J. Uszkoreit, L. Jones, A. N. Gomez, L. Kaiser, and I. Polosukhin, "Attention is all you need," in *Annu. Conf. Neur. Inform. Process. Syst.*, 2017, pp. 6000–6010.
- [27] X. Zhai, A. Kolesnikov, N. Houlsby, and L. Beyer, "Scaling vision transformers," in *IEEE Conf. Comput. Vis. Pattern Recog.*, 2022, pp. 12 104–12 113.
- [28] L. Meng, H. Li, B.-C. Chen, S. Lan, Z. Wu, Y.-G. Jiang, and S.-N. Lim, "AdaViT: Adaptive vision transformers for efficient image recognition," in *IEEE Conf. Comput. Vis. Pattern Recog.*, 2022, pp. 12 309–12 318.
- [29] Y. Liu, Y.-H. Wu, G. Sun, L. Zhang, A. Chhatkuli, and L. Van Gool, "Vision transformers with hierarchical attention," *Machine Intelligence Research*, vol. 21, no. 4, pp. 670–683, 2024.
- [30] Z. Liu, H. Hu, Y. Lin, Z. Yao, Z. Xie, Y. Wei, J. Ning, Y. Cao, Z. Zhang, L. Dong *et al.*, "Swin transformer v2: Scaling up capacity and resolution," in *IEEE Conf. Comput. Vis. Pattern Recog.*, 2022, pp. 12 009–12 019.
- [31] R. J. Chen, C. Chen, Y. Li, T. Y. Chen, A. D. Trister, R. G. Krishnan, and F. Mahmood, "Scaling vision transformers to gigapixel images via hierarchical self-supervised learning," in *IEEE Conf. Comput. Vis. Pattern Recog.*, 2022, pp. 16 144–16 155.
- [32] S. Yan, X. Xiong, A. Arnab, Z. Lu, M. Zhang, C. Sun, and C. Schmid, "Multiview transformers for video recognition," in *IEEE Conf. Comput. Vis. Pattern Recog.*, 2022, pp. 3333–3343.
- [33] J. Gu, H. Kwon, D. Wang, W. Ye, M. Li, Y.-H. Chen, L. Lai, V. Chandra, and D. Z. Pan, "Multi-scale high-resolution vision transformer for semantic segmentation," in *IEEE Conf. Comput. Vis. Pattern Recog.*, 2022, pp. 12 094–12 103.
- [34] X. Ding, Y. Zhang, Y. Ge, S. Zhao, L. Song, X. Yue, and Y. Shan, "UniRepLKNet: A universal perception large-kernel ConvNet for audio video point cloud time-series and image recognition," in *IEEE Conf. Comput. Vis. Pattern Recog.*, 2024, pp. 5513–5524.
- [35] Y.-H. Wu, Y. Liu, X. Zhan, and M.-M. Cheng, "P2T: Pyramid pooling transformer for scene understanding," *IEEE Trans. Pattern Anal. Mach. Intell.*, vol. 45, no. 11, pp. 12 760–12 771, 2022.
- [36] A. Dosovitskiy, L. Beyer, A. Kolesnikov, D. Weissenborn, X. Zhai, T. Unterthiner, M. Dehghani, M. Minderer, G. Heigold, S. Gelly, J. Uszkoreit, and N. Houlsby, "An image is worth 16x16 words: Transformers for image recognition at scale," in *Int. Conf. Learn. Represent.*, 2021.
- [37] N. Carion, F. Massa, G. Synnaeve, N. Usunier, A. Kirillov, and S. Zagoruyko, "End-to-end object detection with transformers," in *Eur. Conf. Comput. Vis.*, 2020, pp. 213–229.
- [38] P. Voigtlaender, M. Krause, A. Osep, J. Luiten, B. B. G. Sekar, A. Geiger, and B. Leibe, "MOTS: Multi-object tracking and segmentation," in *IEEE Conf. Comput. Vis. Pattern Recog.*, 2019, pp. 7942–7951.
- [39] H. K. Cheng, S. W. Oh, B. Price, A. Schwing, and J.-Y. Lee, "Tracking anything with decoupled video segmentation," in *Int. Conf. Comput. Vis.*, 2023, pp. 1316–1326.
- [40] A. Radford, J. W. Kim, C. Hallacy, A. Ramesh, G. Goh, S. Agarwal, G. Sastry, A. Askell, P. Mishkin, J. Clark *et al.*, "Learning transferable visual models from natural language supervision," in *Int. Conf. Mach. Learn.*, 2021, pp. 8748–8763.
- [41] K. Han, Y. Liu, J. H. Liew, H. Ding, J. Liu, Y. Wang, Y. Tang, Y. Yang, J. Feng, Y. Zhao *et al.*, "Global knowledge calibration for fast open-vocabulary segmentation," in *Int. Conf. Comput. Vis.*, 2023, pp. 797–807.
- [42] H. Zhang, F. Li, X. Zou, S. Liu, C. Li, J. Yang, and L. Zhang, "A simple framework for open-vocabulary segmentation and detection," in *Int. Conf. Comput. Vis.*, 2023, pp. 1020–1031.
- [43] J. Xu, J. Hou, Y. Zhang, R. Feng, Y. Wang, Y. Qiao, and W. Xie, "Learning open-vocabulary semantic segmentation models from natural language supervision," in *IEEE Conf. Comput. Vis. Pattern Recog.*, 2023, pp. 2935–2944.
- [44] C. Han, Y. Zhong, D. Li, K. Han, and L. Ma, "Open-vocabulary semantic segmentation with decoupled one-pass network," in *Int. Conf. Comput. Vis.*, 2023, pp. 1086–1096.
- [45] X. Chen, S. Li, S.-N. Lim, A. Torralba, and H. Zhao, "Open-vocabulary panoptic segmentation with embedding modulation," in *Int. Conf. Comput. Vis.*, 2023, pp. 1141–1150.
- [46] W. Wang, T. Zhou, F. M. Porikli, D. J. Crandall, and L. V. Gool, "A survey on deep learning technique for video segmentation," in *IEEE Trans. Pattern Anal. Mach. Intell.*, vol. 45, no. 6, IEEE, 2022, pp. 7099–7122.
- [47] X. Li, H. Ding, W. Zhang, H. Yuan, J. Pang, G. Cheng, K. Chen, Z. Liu, and C. C. Loy, "Transformer-based visual segmentation: A survey," in *IEEE Trans. Pattern Anal. Mach. Intell.*, vol. 46, no. 12, IEEE, 2024, pp. 10 138–10 163.
- [48] J. Miao, X. Wang, Y. Wu, W. Li, X. Zhang, Y. Wei, and Y. Yang, "Large-scale video panoptic segmentation in the wild: A benchmark," in *IEEE Conf. Comput. Vis. Pattern Recog.*, 2022, pp. 21 001–21 011.
- [49] P. E. DO CT OR OF, "Machine perception of three-dimensional, so lids," Ph.D. dissertation, PhD thesis, MASSACHUSETTS INSTITUTE OF TECHNOLOGY, 1961.
- [50] C. Xu and J. J. Corso, "Evaluation of super-voxel methods for early video processing," in *IEEE Conf. Comput. Vis. Pattern Recog.*, 2012, pp. 1202–1209.
- [51] J. Chang, D. Wei, and J. W. Fisher, "A video representation using temporal superpixels," in *IEEE Conf. Comput. Vis. Pattern Recog.*, 2013, pp. 2051–2058.
- [52] P. Ochs, J. Malik, and T. Brox, "Segmentation of moving objects by long term video analysis," *IEEE Trans. Pattern Anal. Mach. Intell.*, vol. 36, no. 6, pp. 1187–1200, 2013.
- [53] A. Papazoglou and V. Ferrari, "Fast object segmentation in unconstrained video," in *Int. Conf. Comput. Vis.*, 2013, pp. 1777–1784.
- [54] M. Narayana, A. Hanson, and E. Learned-Miller, "Coherent motion segmentation in moving camera videos using optical flow orientations," in *Int. Conf. Comput. Vis.*, 2013, pp. 1577–1584.
- [55] D. Sun, E. B. Sudderth, and M. J. Black, "Layered segmentation and optical flow estimation over time," in *IEEE Conf. Comput. Vis. Pattern Recog.* IEEE, 2012, pp. 1768–1775.
- [56] X. Bai, J. Wang, and G. Sapiro, "Dynamic color flow: A motion-adaptive color model for object segmentation in video," in *Eur. Conf. Comput. Vis.*, 2010, pp. 617–630.
- [57] S. Liu, L. Yuan, P. Tan, and J. Sun, "Steadyflow: Spatially smooth optical flow for video stabilization," in *IEEE Conf. Comput. Vis. Pattern Recog.*, 2014, pp. 4209–4216.
- [58] A. Khoreva, F. Galasso, M. Hein, and B. Schiele, "Classifier based graph construction for video segmentation," in *IEEE Conf. Comput. Vis. Pattern Recog.*, 2015, pp. 951–960.
- [59] Y. Peng, L. Chen, F.-X. Ou-Yang, W. Chen, and J.-H. Yong, "Jf-cut: A parallel graph cut approach for large-scale image and video," *IEEE Trans. Image Process.*, vol. 24, no. 2, pp. 655–666, 2014.
- [60] X. Jin, X. Li, H. Xiao, X. Shen, Z. Lin, J. Yang, Y. Chen, J. Dong, L. Liu, Z. Jie *et al.*, "Video scene parsing with predictive feature learning," in *Int. Conf. Comput. Vis.*, 2017, pp. 5580–5588.
- [61] W. Yuan, X. Gu, Z. Dai, S. Zhu, and P. Tan, "Neural window fully-connected CRFs for monocular depth estimation," in *IEEE Conf. Comput. Vis. Pattern Recog.*, 2022, pp. 3916–3925.
- [62] L. Yang, Y. Fan, and N. Xu, "Video instance segmentation," in *Int. Conf. Comput. Vis.*, 2019, pp. 5187–5196.
- [63] L.-C. Chen, R. G. Lopes, B. Cheng, M. D. Collins, E. D. Cubuk, B. Zoph, H. Adam, and J. Shlens, "Naive-Student: Leveraging semi-supervised learning in video sequences for urban scene segmentation," in *Eur. Conf. Comput. Vis.*, 2020, pp. 695–714.
- [64] L. Hoyer, D. Dai, Y. Chen, A. Köring, S. Saha, and L. V. Gool, "Three ways to improve semantic segmentation with self-supervised depth estimation," in *IEEE Conf. Comput. Vis. Pattern Recog.*, 2020, pp. 11 125–11 135.
- [65] J. Lao, W. Hong, X. Guo, Y. Zhang, J. Wang, J. Chen, and W. Chu, "Simultaneously short- and long-term temporal modeling for semi-supervised video semantic segmentation," in *IEEE Conf. Comput. Vis. Pattern Recog.*, 2023, pp. 14 763–14 772.

- [66] E. Shelhamer, K. Rakelly, J. Hoffman, and T. Darrell, "Clockwork convnets for video semantic segmentation," in *Eur. Conf. Comput. Vis.*, 2016, pp. 852–868.
- [67] H. Park, A. Yessenbayev, T. Singhal, N. K. Adhikari, Y. Zhang, S. M. Borse, H. Cai, N. P. Pandey, F. Yin, F. Mayer *et al.*, "Real-time, accurate, and consistent video semantic segmentation via unsupervised adaptation and cross-unit deployment on mobile device," in *IEEE Conf. Comput. Vis. Pattern Recog.*, 2022, pp. 21 431–21 438.
- [68] Y.-S. Xu, T.-J. Fu, H.-K. Yang, and C.-Y. Lee, "Dynamic video segmentation network," in *IEEE Conf. Comput. Vis. Pattern Recog.*, 2018, pp. 6556–6565.
- [69] Y. Li, J. Shi, and D. Lin, "Low-latency video semantic segmentation," in *IEEE Conf. Comput. Vis. Pattern Recog.*, 2018, pp. 5997–6005.
- [70] G. Sun, Y. Liu, H. Ding, T. Probst, and L. van Gool, "Coarse-to-fine feature mining for video semantic segmentation," in *IEEE Conf. Comput. Vis. Pattern Recog.*, 2022, pp. 3116–3127.
- [71] G. Sun, Y. Liu, H. Tang, A. Chhatkuli, L. Zhang, and L. Van Gool, "Mining relations among cross-frame affinities for video semantic segmentation," in *Eur. Conf. Comput. Vis.*, 2022, pp. 522–539.
- [72] P. Luo, G. Wang, L. Lin, and X. Wang, "Deep dual learning for semantic image segmentation," in *Int. Conf. Comput. Vis.*, 2017, pp. 2718–2726.
- [73] J. Ahn and S. Kwak, "Learning pixel-level semantic affinity with image-level supervision for weakly supervised semantic segmentation," in *IEEE Conf. Comput. Vis. Pattern Recog.*, 2018, pp. 4981–4990.
- [74] K. Wang, J. H. Liew, Y. Zou, D. Zhou, and J. Feng, "PANet: Few-shot image semantic segmentation with prototype alignment," in *Int. Conf. Comput. Vis.*, 2019, pp. 9197–9206.
- [75] N. Araslanov and S. Roth, "Single-stage semantic segmentation from image labels," in *IEEE Conf. Comput. Vis. Pattern Recog.*, 2020, pp. 4253–4262.
- [76] J. Fan, Z. Zhang, T. Tan, C. Song, and J. Xiao, "CIAN: Cross-image affinity net for weakly supervised semantic segmentation," in *AAAI Conf. Artif. Intell.*, 2020, pp. 10762–10769.
- [77] B. Mahasseni, S. Todorovic, and A. Fern, "Budget-aware deep semantic video segmentation," in *IEEE Conf. Comput. Vis. Pattern Recog.*, 2017, pp. 1029–1038.
- [78] M. Siam, S. Valipour, M. Jagersand, and N. Ray, "Convolutional gated recurrent networks for video segmentation," in *Int. Conf. Image Process.*, 2017, pp. 3090–3094.
- [79] S. Caelles, K.-K. Maninis, J. Pont-Tuset, L. Leal-Taixé, D. Cremers, and L. Van Gool, "One-shot video object segmentation," in *IEEE Conf. Comput. Vis. Pattern Recog.*, 2017, pp. 221–230.
- [80] S. W. Oh, J.-Y. Lee, N. Xu, and S. J. Kim, "Space-time memory networks for video object segmentation with user guidance," *IEEE Trans. Pattern Anal. Mach. Intell.*, vol. 44, no. 1, pp. 442–455, 2020.
- [81] F. Perazzi, A. Khoreva, R. Benenson, B. Schiele, and A. Sorkine-Hornung, "Learning video object segmentation from static images," in *IEEE Conf. Comput. Vis. Pattern Recog.*, 2017, pp. 2663–2672.
- [82] C. Ventura, M. Bellver, A. Girbau, A. Salvador, F. Marques, and X. Giro-i Nieto, "RVOS: End-to-end recurrent network for video object segmentation," in *IEEE Conf. Comput. Vis. Pattern Recog.*, 2019, pp. 5277–5286.
- [83] H. K. Cheng, S. W. Oh, B. Price, J.-Y. Lee, and A. Schwing, "Putting the object back into video object segmentation," in *IEEE Conf. Comput. Vis. Pattern Recog.*, 2024, pp. 3151–3161.
- [84] X. Zhu, J. Dai, L. Yuan, and Y. Wei, "Towards high performance video object detection," in *IEEE Conf. Comput. Vis. Pattern Recog.*, 2018, pp. 7210–7218.
- [85] X. Zhu, Y. Wang, J. Dai, L. Yuan, and Y. Wei, "Flow-guided feature aggregation for video object detection," in *Int. Conf. Comput. Vis.*, 2017, pp. 408–417.
- [86] S. Wang, Y. Zhou, J. Yan, and Z. Deng, "Fully motion-aware network for video object detection," in *Eur. Conf. Comput. Vis.*, 2018, pp. 542–557.
- [87] G. Sun, Y. Hua, G. Hu, and N. Robertson, "Mamba: Multi-level aggregation via memory bank for video object detection," in *AAAI Conf. Artif. Intell.*, 2021, pp. 2620–2627.
- [88] M. Zhang, J. Liu, Y. Wang, Y. Piao, S. Yao, W. Ji, J. Li, H. Lu, and Z. Luo, "Dynamic context-sensitive filtering network for video salient object detection," in *Int. Conf. Comput. Vis.*, 2021, pp. 1553–1563.
- [89] M. N. Meeran, B. P. Mantha *et al.*, "SAM-PM: Enhancing video camouflaged object detection using spatio-temporal attention," in *IEEE Conf. Comput. Vis. Pattern Recog.*, 2024, pp. 1857–1866.
- [90] S. Chandra, C. Couprie, and I. Kokkinos, "Deep spatio-temporal random fields for efficient video segmentation," in *IEEE Conf. Comput. Vis. Pattern Recog.*, 2018, pp. 8915–8924.
- [91] F. Perazzi, J. Pont-Tuset, B. McWilliams, L. Van Gool, M. Gross, and A. Sorkine-Hornung, "A benchmark dataset and evaluation methodology for video object segmentation," in *IEEE Conf. Comput. Vis. Pattern Recog.*, 2016, pp. 724–732.
- [92] J. Pont-Tuset, F. Perazzi, S. Caelles, P. Arbeláez, A. Sorkine-Hornung, and L. Van Gool, "The 2017 DAVIS challenge on video object segmentation," *arXiv preprint arXiv:1704.00675*, 2017.
- [93] G. J. Brostow, J. Shotton, J. Fauqueur, and R. Cipolla, "Segmentation and recognition using structure from motion point clouds," in *Eur. Conf. Comput. Vis.*, 2008, pp. 44–57.
- [94] M. Cordts, M. Omran, S. Ramos, T. Rehfeld, M. Enzweiler, R. Benenson, U. Franke, S. Roth, and B. Schiele, "The Cityscapes dataset for semantic urban scene understanding," in *IEEE Conf. Comput. Vis. Pattern Recog.*, 2016, pp. 3213–3223.
- [95] D. Nilsson and C. Sminchisescu, "Semantic video segmentation by gated recurrent flow propagation," in *IEEE Conf. Comput. Vis. Pattern Recog.*, 2018, pp. 6819–6828.
- [96] A. Geiger, P. Lenz, and R. Urtasun, "Are we ready for autonomous driving? the KITTI vision benchmark suite," in *IEEE Conf. Comput. Vis. Pattern Recog.*, 2012, pp. 3354–3361.
- [97] M. Ding, Z. Wang, B. Zhou, J. Shi, Z. Lu, and P. Luo, "Every frame counts: Joint learning of video segmentation and optical flow," in *AAAI Conf. Artif. Intell.*, 2020, pp. 10713–10720.
- [98] P. Hu, F. C. Heilbron, O. Wang, Z. L. Lin, S. Sclaroff, and F. Perazzi, "Temporally distributed networks for fast video semantic segmentation," in *IEEE Conf. Comput. Vis. Pattern Recog.*, 2020, pp. 8815–8824.
- [99] N. Silberman, D. Hoiem, P. Kohli, and R. Fergus, "Indoor segmentation and support inference from RGBD images," in *Eur. Conf. Comput. Vis.*, 2012, pp. 746–760.
- [100] Y. Liu, C. Shen, C. Yu, and J. Wang, "Efficient semantic video segmentation with per-frame inference," in *Eur. Conf. Comput. Vis.*, 2020, pp. 352–368.
- [101] J. Miao, Y. Wei, Y. Wu, C. Liang, G. Li, and Y. Yang, "VSPW: A large-scale dataset for video scene parsing in the wild," in *IEEE Conf. Comput. Vis. Pattern Recog.*, 2021, pp. 4133–4143.
- [102] C. Yang, H. Zhou, Z. An, X. Jiang, Y. Xu, and Q. Zhang, "Cross-image relational knowledge distillation for semantic segmentation," in *IEEE Conf. Comput. Vis. Pattern Recog.*, 2022, pp. 12 309–12 318.
- [103] M. Everingham, S. A. Eslami, L. Van Gool, C. K. Williams, J. Winn, and A. Zisserman, "The pascal visual object classes challenge: A retrospective," *Int. J. Comput. Vis.*, vol. 111, no. 1, pp. 98–136, 2015.
- [104] J. Zhuang, Z. Wang, and Y. Gao, "Semi-supervised video semantic segmentation with inter-frame feature reconstruction," in *IEEE Conf. Comput. Vis. Pattern Recog.*, 2022, pp. 3263–3271.
- [105] W. Ji, J. Li, C. Bian, Z. Zhou, J. Zhao, A. L. Yuille, and L. Cheng, "Multispectral video semantic segmentation: A benchmark dataset and baseline," in *IEEE Conf. Comput. Vis. Pattern Recog.*, 2023, pp. 1094–1104.
- [106] Y. Weng, M. Han, H. He, M. Li, L. Yao, X. Chang, and B. Zhuang, "Mask propagation for efficient video semantic segmentation," in *Annu. Conf. Neur. Inform. Process. Syst.*, 2023, pp. 7170–7183.
- [107] C. Yang, P. Zhao, Y. Li, W. Niu, J. Guan, H. Tang, M. Qin, B. Ren, X. Lin, and Y. Wang, "Pruning parameterization with bi-level optimization for efficient semantic segmentation on the edge," in *IEEE Conf. Comput. Vis. Pattern Recog.*, 2023, pp. 15 402–15 412.
- [108] B. Zhou, H. Zhao, X. Puig, T. Xiao, S. Fidler, A. Barriuso, and A. Torralba, "Semantic understanding of scenes through the ADE20K dataset," *Int. J. Comput. Vis.*, vol. 127, no. 3, pp. 302–321, 2019.
- [109] D. Guo, D.-P. Fan, T. Lu, C. Sakaridis, and L. V. Gool, "Vanishing-point-guided video semantic segmentation of driving scenes," in *IEEE Conf. Comput. Vis. Pattern Recog.*, 2024, pp. 3544–3553.
- [110] C. Sakaridis, D. Dai, and L. Van Gool, "ACDC: The adverse conditions dataset with correspondences for semantic driving scene understanding," in *Int. Conf. Comput. Vis.*, 2021, pp. 10 745–10 755.
- [111] J. Zhuang, Z. Wang, Y. Zhang, and Z. Fan, "Infer from what you have seen before: Temporally-dependent classifier for semi-supervised video segmentation," in *IEEE Conf. Comput. Vis. Pattern Recog.*, 2024, pp. 3575–3584.
- [112] G. Sun, Y. Liu, H. Ding, M. Wu, and L. V. Gool, "Learning local and global temporal contexts for video semantic segmentation," *IEEE Trans. Pattern Anal. Mach. Intell.*, vol. 46, no. 10, pp. 6919–6934, 2024.
- [113] S. A. S. Hesham, Y. Liu, G. Sun, H. Ding, J. Yang, E. Konukoglu, X. Geng, and X. Jiang, "Exploiting temporal state space sharing for video semantic segmentation," in *IEEE Conf. Comput. Vis. Pattern Recog.*, 2025.

- [114] L. Jiao, R. Zhang, F. Liu, S. Yang, B. Hou, L. Li, and X. Tang, "New generation deep learning for video object detection: A survey," *IEEE Trans. Neur. Net. Learn. Syst.*, vol. 33, no. 8, pp. 3195–3215, 2021.
- [115] A. Athar, S. Mahadevan, A. Osep, L. Leal-Taixé, and B. Leibe, "STEm-Seg: Spatio-temporal embeddings for instance segmentation in videos," in *Eur. Conf. Comput. Vis.*, 2020, pp. 158–177.
- [116] G. Bertasius and L. Torresani, "Classifying, segmenting, and tracking object instances in video with mask propagation," in *IEEE Conf. Comput. Vis. Pattern Recog.*, 2020, pp. 9739–9748.
- [117] C.-C. Lin, Y. Hung, R. Feris, and L. He, "Video instance segmentation tracking with a modified VAE architecture," in *IEEE Conf. Comput. Vis. Pattern Recog.*, 2020, pp. 13 147–13 157.
- [118] L. Porzi, M. Hofinger, I. Ruiz, J. Serrat, S. R. Bulò, and P. Kotschieder, "Learning multi-object tracking and segmentation from automatic annotations," in *IEEE Conf. Comput. Vis. Pattern Recog.*, 2019, pp. 6845–6854.
- [119] F. Yu, H. Chen, X. Wang, W. Xian, Y. Chen, F. Liu, V. Madhavan, and T. Darrell, "BDD100K: A diverse driving dataset for heterogeneous multitask learning," in *IEEE Conf. Comput. Vis. Pattern Recog.*, 2020, pp. 2636–2645.
- [120] Y. Fu, S. Liu, U. Iqbal, S. D. Mello, H. Shi, and J. Kautz, "Learning to track instances without video annotations," in *IEEE Conf. Comput. Vis. Pattern Recog.*, 2021, pp. 8676–8685.
- [121] Y. Fu, L. Yang, D. Liu, T. S. Huang, and H. Shi, "CompFeat: Comprehensive feature aggregation for video instance segmentation," in *AAAI Conf. Artif. Intell.*, vol. 35, no. 2, 2021, pp. 1361–1369.
- [122] S. Hwang, M. Heo, S. W. Oh, and S. J. Kim, "Video instance segmentation using inter-frame communication transformers," in *Annu. Conf. Neur. Inform. Process. Syst.*, 2021, pp. 13 352–13 363.
- [123] H. Lin, R. Wu, S. Liu, J. Lu, and J. Jia, "Video instance segmentation with a propose-reduce paradigm," in *Int. Conf. Comput. Vis.*, 2021, pp. 1739–1748.
- [124] D. Liu, Y. Cui, W. Tan, and Y. Chen, "SG-Net: Spatial granularity network for one-stage video instance segmentation," in *IEEE Conf. Comput. Vis. Pattern Recog.*, 2021, pp. 9816–9825.
- [125] Q. Liu, V. Ramanathan, D. K. Mahajan, A. L. Yuille, and Z. Yang, "Weakly supervised instance segmentation for videos with temporal mask consistency," in *IEEE Conf. Comput. Vis. Pattern Recog.*, 2021, pp. 13 963–13 973.
- [126] Y. Wang, Z. Xu, X. Wang, C. Shen, B. Cheng, H. Shen, and H. Xia, "End-to-end video instance segmentation with transformers," in *IEEE Conf. Comput. Vis. Pattern Recog.*, 2021, pp. 8741–8750.
- [127] J. Wu, J. Cao, L. Song, Y. Wang, M. Yang, and J. Yuan, "Track to detect and segment: An online multi-object tracker," in *IEEE Conf. Comput. Vis. Pattern Recog.*, 2021, pp. 12 347–12 356.
- [128] S. Yang, Y. Fang, X. Wang, Y. Li, C. Fang, Y. Shan, B. Feng, and W. Liu, "Crossover learning for fast online video instance segmentation," in *Int. Conf. Comput. Vis.*, 2021, pp. 8043–8052.
- [129] J. Qi, Y. Gao, Y. Hu, X. Wang, X. Liu, X. Bai, S. J. Belongie, A. L. Yuille, P. H. S. Torr, and S. Bai, "Occluded video instance segmentation: A benchmark," in *Int. J. Comput. Vis.*, vol. 130, no. 8. Springer, 2022, pp. 2022–2039.
- [130] X. Li, H. He, Y. Yang, H. Ding, K. Yang, G. Cheng, Y. Tong, and D. Tao, "Improving video instance segmentation via temporal pyramid routing," *IEEE Trans. Pattern Anal. Mach. Intell.*, vol. 45, no. 5, pp. 6594–6601, 2022.
- [131] S. H. Han, S. Hwang, S. W. Oh, Y. Park, H. Kim, M.-J. Kim, and S. J. Kim, "VISOLO: Grid-based space-time aggregation for efficient online video instance segmentation," in *IEEE Conf. Comput. Vis. Pattern Recog.*, 2022, pp. 2896–2905.
- [132] T.-Y. Lin, M. Maire, S. Belongie, J. Hays, P. Perona, D. Ramanan, P. Dollár, and C. L. Zitnick, "Microsoft coco: Common objects in context," in *Eur. Conf. Comput. Vis.*, 2014, pp. 740–755.
- [133] D.-A. Huang, Z. Yu, and A. Anandkumar, "MinVIS: A minimal video instance segmentation framework without video-based training," in *Annu. Conf. Neur. Inform. Process. Syst.*, 2022, pp. 31 265–31 277.
- [134] Z. Jiang, Z. Gu, J. Peng, H. Zhou, L. Liu, Y. Wang, Y. Tai, C. Wang, and L. Zhang, "STC: Spatio-temporal contrastive learning for video instance segmentation," in *Eur. Conf. Comput. Vis.*, 2022, pp. 539–556.
- [135] T. Meinhardt, A. Kirillov, L. Leal-Taixé, and C. Feichtenhofer, "TrackFormer: Multi-object tracking with transformers," in *IEEE Conf. Comput. Vis. Pattern Recog.*, 2022, pp. 8844–8854.
- [136] A. Milan, L. Leal-Taixé, I. Reid, S. Roth, and K. Schindler, "MOT16: A benchmark for multi-object tracking," *arXiv preprint arXiv:1603.00831*, 2016.
- [137] J. Wu, Y. Jiang, S. Bai, W. Zhang, and X. Bai, "SeqFormer: Sequential transformer for video instance segmentation," in *Eur. Conf. Comput. Vis.*, 2022, pp. 553–569.
- [138] J. Wu, Q. Liu, Y. Jiang, S. Bai, A. Yuille, and X. Bai, "In defense of online models for video instance segmentation," in *Eur. Conf. Comput. Vis.*, 2022, pp. 588–605.
- [139] S. Yang, X. Wang, Y. Li, Y. Fang, J. Fang, W. Liu, X. Zhao, and Y. Shan, "Temporally efficient vision transformer for video instance segmentation," in *IEEE Conf. Comput. Vis. Pattern Recog.*, 2022, pp. 2885–2895.
- [140] M. Heo, S. Hwang, J. Hyun, H. Kim, S. W. Oh, J.-Y. Lee, and S. J. Kim, "A generalized framework for video instance segmentation," in *IEEE Conf. Comput. Vis. Pattern Recog.*, 2023, pp. 14 623–14 632.
- [141] X. Wang, I. Misra, Z. Zeng, R. Girdhar, and T. Darrell, "VideoCutLER: Surprisingly simple unsupervised video instance segmentation," in *IEEE Conf. Comput. Vis. Pattern Recog.*, 2023, pp. 22 755–22 764.
- [142] K. Ying, Q. Zhong, W. Mao, Z. Wang, H. Chen, L. Y. Wu, Y. Liu, C. Fan, Y. Zhuge, and C. Shen, "CTVIS: Consistent training for online video instance segmentation," in *Int. Conf. Comput. Vis.*, 2023, pp. 899–908.
- [143] T. Zhang, X. Tian, Y. Wu, S. Ji, X. Wang, Y. Zhang, and P. Wan, "Dvis: Decoupled video instance segmentation framework," in *Int. Conf. Comput. Vis.*, 2023, pp. 1282–1291.
- [144] H. Fang, P. Wu, Y. Li, X. Zhang, and X. Lu, "Unified embedding alignment for open-vocabulary video instance segmentation," in *Eur. Conf. Comput. Vis.*, 2024, pp. 225–241.
- [145] H. Wang, C. Yan, S. Wang, X. Jiang, X. Tang, Y. Hu, W. Xie, and E. Gavves, "Towards open-vocabulary video instance segmentation," in *Int. Conf. Comput. Vis.*, 2023, pp. 4057–4066.
- [146] H. Wang, C. Yan, K. Chen, X. Jiang, X. Tang, Y. Hu, G. Kang, W. Xie, and E. Gavves, "OV-VIS: Open-vocabulary video instance segmentation," *Int. J. Comput. Vis.*, vol. 132, no. 11, pp. 5048–5065, 2024.
- [147] A. Gupta, P. Dollar, and R. Girshick, "LVIS: A dataset for large vocabulary instance segmentation," in *IEEE Conf. Comput. Vis. Pattern Recog.*, 2019, pp. 5356–5364.
- [148] D. Kim, S. Woo, J.-Y. Lee, and I.-S. Kweon, "Video panoptic segmentation," in *IEEE Conf. Comput. Vis. Pattern Recog.*, 2020, pp. 9856–9865.
- [149] S. Qiao, Y. Zhu, H. Adam, A. L. Yuille, and L.-C. Chen, "ViP-DeepLab: Learning visual perception with depth-aware video panoptic segmentation," in *IEEE Conf. Comput. Vis. Pattern Recog.*, 2020, pp. 3996–4007.
- [150] S. Woo, D. Kim, J.-Y. Lee, and I. S. Kweon, "Learning to associate every segment for video panoptic segmentation," in *IEEE Conf. Comput. Vis. Pattern Recog.*, 2021, pp. 2705–2714.
- [151] J. Mei, A. Z. Zhu, X. Yan, H. Yan, S. Qiao, Y. Zhu, L.-C. Chen, H. Kretschmar, and D. Anguelov, "Waymo open dataset: Panoramic video panoptic segmentation," in *Eur. Conf. Comput. Vis.*, 2022, pp. 53–72.
- [152] X. Li, W. Zhang, J. Pang, K. Chen, G. Cheng, Y. Tong, and C. C. Loy, "Video K-Net: A simple, strong, and unified baseline for video segmentation," in *IEEE Conf. Comput. Vis. Pattern Recog.*, 2022, pp. 18 847–18 857.
- [153] X. Li, H. Yuan, W. Zhang, G. Cheng, J. Pang, and C. C. Loy, "Tube-Link: A flexible cross tube framework for universal video segmentation," in *Int. Conf. Comput. Vis.*, 2023, pp. 13 923–13 933.
- [154] H. Yuan, X. Li, Y. Yang, G. Cheng, J. Zhang, Y. Tong, L. Zhang, and D. Tao, "PolyphonicFormer: Unified query learning for depth-aware video panoptic segmentation," in *Eur. Conf. Comput. Vis.*, 2022, pp. 582–599.
- [155] J. Xu, S. Liu, A. Vahdat, W. Byeon, X. Wang, and S. De Mello, "Open-vocabulary panoptic segmentation with text-to-image diffusion models," in *IEEE Conf. Comput. Vis. Pattern Recog.*, 2023, pp. 2955–2966.
- [156] H. Caesar, J. Uijlings, and V. Ferrari, "COCO-Stuff: Thing and stuff classes in context," in *IEEE Conf. Comput. Vis. Pattern Recog.*, 2018, pp. 1209–1218.
- [157] Z. Xu, W. Zhang, X. Tan, W. Yang, H. Huang, S. Wen, E. Ding, and L. Huang, "Segment as points for efficient online multi-object tracking and segmentation," in *Eur. Conf. Comput. Vis.*, 2020, pp. 264–281.
- [158] A. Choudhuri, G. Chowdhary, and A. G. Schwing, "Assignment-space-based multi-object tracking and segmentation," in *Int. Conf. Comput. Vis.*, 2021, pp. 13 598–13 607.
- [159] G. Brasó, O. Cetintas, and L. Leal-Taixé, "Multi-object tracking and segmentation via neural message passing," *Int. J. Comput. Vis.*, vol. 130, no. 12, pp. 3035–3053, 2022.
- [160] P. Dendorfer, H. Rezatofighi, A. Milan, J. Shi, D. Cremers, I. Reid, S. Roth, K. Schindler, and L. Leal-Taixé, "MOT20: A bench-

- mark for multi object tracking in crowded scenes,” *arXiv preprint arXiv:2003.09003*, 2020.
- [161] W. Lin, H. Liu, S. Liu, Y. Li, R. Qian, T. Wang, N. Xu, H. Xiong, G.-J. Qi, and N. Sebe, “Human in events: A large-scale benchmark for human-centric video analysis in complex events,” *arXiv preprint arXiv:2005.04490*, 2020.
- [162] Y. Xu, Z. Yang, and Y. Yang, “Integrating boxes and masks: A multi-object framework for unified visual tracking and segmentation,” in *Int. Conf. Comput. Vis.*, 2023, pp. 9738–9751.
- [163] N. Xu, L. Yang, Y. Fan, D. Yue, Y. Liang, J. Yang, and T. Huang, “YouTube-VOS: A large-scale video object segmentation benchmark,” *arXiv preprint arXiv:1809.03327*, 2018.
- [164] Y. Cheng, L. Li, Y. Xu, X. Li, Z. Yang, W. Wang, and Y. Yang, “Segment and track anything,” *arXiv preprint arXiv:2305.06558*, 2023.
- [165] F. Rajič, L. Ke, Y.-W. Tai, C.-K. Tang, M. Danelljan, and F. Yu, “Segment anything meets point tracking,” *arXiv preprint arXiv:2307.01197*, 2023.
- [166] N. Ravi, V. Gabeur, Y.-T. Hu, R. Hu, C. Ryali, T. Ma, H. Khedr, R. Rädle, C. Rolland, L. Gustafson *et al.*, “SAM 2: Segment anything in images and videos,” *arXiv preprint arXiv:2408.00714*, 2024.
- [167] A. Kirillov, E. Mintun, N. Ravi, H. Mao, C. Rolland, L. Gustafson, T. Xiao, S. Whitehead, A. C. Berg, W.-Y. Lo *et al.*, “Segment anything,” in *Int. Conf. Comput. Vis.*, 2023, pp. 4015–4026.
- [168] S. Liu, Z. Zeng, T. Ren, F. Li, H. Zhang, J. Yang, Q. Jiang, C. Li, J. Yang, H. Su *et al.*, “Grounding DINO: Marrying DINO with grounded pre-training for open-set object detection,” in *Eur. Conf. Comput. Vis.*, 2024, pp. 38–55.
- [169] W. Zhu, J. Cao, J. Xie, S. Yang, and Y. Pang, “CLIP-VIS: Adapting CLIP for open-vocabulary video instance segmentation,” *IEEE Trans. Circ. Syst. Video Technol.*, vol. 35, no. 2, pp. 1098–1110, 2025.
- [170] X. Li, Y. Liu, G. Sun, M. Wu, L. Zhang, and C. Zhu, “Towards open-vocabulary video semantic segmentation,” *IEEE Trans. Multimedia*, 2025.
- [171] M. Weber, J. Xie, M. D. Collins, Y. Zhu, P. Voigtlaender, H. Adam, B. Green, A. Geiger, B. Leibe, D. Cremers, A. Osep, L. Leal-Taixé, and L.-C. Chen, “STEP: Segmenting and tracking every pixel,” in *NeurIPS Datasets and Benchmarks*, 2021.
- [172] D. Kim, J. Xie, H. Wang, S. Qiao, Q. Yu, H.-S. Kim, H. Adam, I. S. Kweon, and L.-C. Chen, “Tubeformer-DeepLab: Video mask transformer,” in *IEEE Conf. Comput. Vis. Pattern Recog.*, 2022, pp. 13914–13924.
- [173] Y. Zhou, H. Zhang, H. Lee, S. Sun, P. Li, Y. Zhu, B. Yoo, X. Qi, and J.-J. Han, “Slot-VPS: Object-centric representation learning for video panoptic segmentation,” in *IEEE Conf. Comput. Vis. Pattern Recog.*, 2022, pp. 3093–3103.
- [174] A. Osep, W. Mehner, M. Mathias, and B. Leibe, “Combined image- and world-space tracking in traffic scenes,” in *IEEE Int. Conf. Robot. Autom.*, 2017, pp. 1988–1995.
- [175] J. Luiten, T. Fischer, and B. Leibe, “Track to reconstruct and reconstruct to track,” *IEEE Trans. Robot. Autom. Let.*, vol. 5, no. 2, pp. 1803–1810, 2020.
- [176] A. Osep, W. Mehner, P. Voigtlaender, and B. Leibe, “Track, then decide: Category-agnostic vision-based multi-object tracking,” in *IEEE Int. Conf. Robot. Autom.*, 2018, pp. 3494–3501.
- [177] W. Wang, M. Feiszli, H. Wang, and D. Tran, “Unidentified video objects: A benchmark for dense, open-world segmentation,” in *Int. Conf. Comput. Vis.*, 2021, pp. 10776–10785.
- [178] J. Wu, X. Li, S. Xu, H. Yuan, H. Ding, Y. Yang, X. Li, J. Zhang, Y. Tong, X. Jiang *et al.*, “Towards open vocabulary learning: A survey,” *IEEE Trans. Pattern Anal. Mach. Intell.*, vol. 46, no. 7, pp. 5092–5113, 2024.
- [179] P. Guo, Z. Zhao, J. Gao, C. Wu, T. He, Z. Zhang, T. Xiao, and W. Zhang, “VideoSAM: Open-world video segmentation,” *arXiv preprint arXiv:2410.08781*, 2024.
- [180] O. Thawakar, S. Narayan, H. Cholakkal, R. M. Anwer, S. Khan, J. Laaksonen, M. Shah, and F. S. Khan, “Video instance segmentation in an open-world,” *Int. J. Comput. Vis.*, vol. 133, no. 1, pp. 398–409, 2025.
- [181] Z. Xue, K. Ashutosh, and K. Grauman, “Learning object state changes in videos: An open-world perspective,” in *IEEE Conf. Comput. Vis. Pattern Recog.*, 2024, pp. 18493–18503.
- [182] L. Tang, P.-T. Jiang, H. Xiao, and B. Li, “Towards training-free open-world segmentation via image prompt foundation models,” *Int. J. Comput. Vis.*, vol. 133, no. 1, pp. 1–15, 2025.
- [183] T. Kalluri, W. Wang, H. Wang, M. Chandraker, L. Torresani, and D. Tran, “Open-world instance segmentation: Top-down learning with bottom-up supervision,” in *IEEE Conf. Comput. Vis. Pattern Recog.*, 2024, pp. 2693–2703.
- [184] A. Athar, J. Luiten, P. Voigtlaender, T. Khurana, A. Dave, B. Leibe, and D. Ramanan, “BURST: A benchmark for unifying object recognition, segmentation and tracking in video,” in *IEEE Winter Conf. App. Comput. Vis.*, 2023, pp. 1674–1683.
- [185] X. Li, H. Yuan, W. Li, H. Ding, S. Wu, W. Zhang, Y. Li, K. Chen, and C. C. Loy, “OMG-Seg: Is one model good enough for all segmentation?” in *IEEE Conf. Comput. Vis. Pattern Recog.*, 2024, pp. 27948–27959.
- [186] M. Chen, L. Li, W. Wang, R. Quan, and Y. Yang, “General and task-oriented video segmentation,” in *Eur. Conf. Comput. Vis.*, 2024, pp. 72–92.
- [187] T. Zhang, X. Li, H. Fei, H. Yuan, S. Wu, S. Ji, C. C. Loy, and S. Yan, “OMG-LLaVA: Bridging image-level, object-level, pixel-level reasoning and understanding,” in *Annu. Conf. Neur. Inform. Process. Syst.*, 2024, pp. 71737–71767.
- [188] Y. Song, Q. Zhou, X. Li, D.-P. Fan, X. Lu, and L. Ma, “BA-SAM: Scalable bias-mode attention mask for segment anything model,” in *IEEE Conf. Comput. Vis. Pattern Recog.*, 2024, pp. 3162–3173.
- [189] X. Yuan, L. Zhou, Z. Sun, Z. Zhou, and J. Lan, “Instruction-guided multi-granularity segmentation and captioning with large multimodal model,” in *AAAI Conf. Artif. Intell.*, 2025, pp. 9725–9733.
- [190] T. Zhang, X. Tian, Y. Zhou, S. Ji, X. Wang, X. Tao, Y. Zhang, P. Wan, Z. Wang, and Y. Wu, “DVIS++: Improved decoupled framework for universal video segmentation,” *IEEE Trans. Pattern Anal. Mach. Intell.*, 2025.
- [191] S. Yan, R. Zhang, Z. Guo, W. Chen, W. Zhang, H. Li, Y. Qiao, H. Dong, Z. He, and P. Gao, “Referred by multi-modality: A unified temporal transformer for video object segmentation,” in *AAAI Conf. Artif. Intell.*, 2024, pp. 6449–6457.
- [192] P. Voigtlaender, S. Changpinyo, J. Pont-Tuset, R. Soricut, and V. Ferrari, “Connecting vision and language with video localized narratives,” in *IEEE Conf. Comput. Vis. Pattern Recog.*, 2023, pp. 2461–2471.
- [193] W. Wang, Z. Chen, X. Chen, J. Wu, X. Zhu, G. Zeng, P. Luo, T. Lu, J. Zhou, Y. Qiao *et al.*, “VisionLLM: Large language model is also an open-ended decoder for vision-centric tasks,” in *Annu. Conf. Neur. Inform. Process. Syst.*, 2023, pp. 61501–61513.
- [194] Z. Li, B. Yang, Q. Liu, Z. Ma, S. Zhang, J. Yang, Y. Sun, Y. Liu, and X. Bai, “Monkey: Image resolution and text label are important things for large multi-modal models,” in *IEEE Conf. Comput. Vis. Pattern Recog.*, 2024, pp. 26763–26773.
- [195] J. Lu, C. Clark, S. Lee, Z. Zhang, S. Khosla, R. Marten, D. Hoiem, and A. Kembhavi, “Unified-IO 2: Scaling autoregressive multimodal models with vision language audio and action,” in *IEEE Conf. Comput. Vis. Pattern Recog.*, 2024, pp. 26439–26455.
- [196] X. Zou, Z.-Y. Dou, J. Yang, Z. Gan, L. Li, C. Li, X. Dai, H. Behl, J. Wang, L. Yuan *et al.*, “Generalized decoding for pixel, image, and language,” in *IEEE Conf. Comput. Vis. Pattern Recog.*, 2023, pp. 15116–15127.
- [197] Y. Zhang, K. Gong, K. Zhang, H. Li, Y. Qiao, W. Ouyang, and X. Yue, “Meta-Transformer: A unified framework for multimodal learning,” *arXiv preprint arXiv:2307.10802*, 2023.
- [198] F. B. Baldassini, M. Shukor, M. Cord, L. Soulier, and B. Piwowarski, “What makes multimodal in-context learning work?” in *IEEE Conf. Comput. Vis. Pattern Recog.*, 2024, pp. 1539–1550.
- [199] T. Srinivasan, T.-Y. Chang, L. Pinto Alva, G. Chochlakis, M. Rostami, and J. Thomason, “CLiMB: A continual learning benchmark for vision-and-language tasks,” in *Annu. Conf. Neur. Inform. Process. Syst.*, 2022, pp. 29440–29453.
- [200] R. Zheng, L. Qi, X. Chen, Y. Wang, K. Wang, Y. Qiao, and H. Zhao, “ViLLa: Video reasoning segmentation with large language model,” *arXiv preprint arXiv:2407.14500*, 2024.
- [201] C. Yan, H. Wang, S. Yan, X. Jiang, Y. Hu, G. Kang, W. Xie, and E. Gavves, “VISA: Reasoning video object segmentation via large language models,” in *Eur. Conf. Comput. Vis.*, 2024, pp. 98–115.
- [202] Z. Bai, T. He, H. Mei, P. Wang, Z. Gao, J. Chen, Z. Zhang, and M. Z. Shou, “One token to seg them all: Language instructed reasoning segmentation in videos,” in *Annu. Conf. Neur. Inform. Process. Syst.*, 2024, pp. 6833–6859.
- [203] S. Gong, Y. Zhuge, L. Zhang, Z. Yang, P. Zhang, and H. Lu, “The devil is in temporal token: High quality video reasoning segmentation,” *arXiv preprint arXiv:2501.08549*, 2025.
- [204] T. Chen, L. Li, S. Saxena, G. Hinton, and D. J. Fleet, “A generalist framework for panoptic segmentation of images and videos,” in *Int. Conf. Comput. Vis.*, 2023, pp. 909–919.

- [205] Z. Gu, H. Chen, and Z. Xu, "DiffusionInst: Diffusion model for instance segmentation," in *IEEE Int. Conf. Acoust. Speech SP*, 2024, pp. 2730–2734.
- [206] L. Qi, L. Yang, W. Guo, Y. Xu, B. Du, V. Jampani, and M.-H. Yang, "UniGS: Unified representation for image generation and segmentation," in *IEEE Conf. Comput. Vis. Pattern Recog.*, 2024, pp. 6305–6315.
- [207] P. Li, C.-W. Xie, H. Xie, L. Zhao, L. Zhang, Y. Zheng, D. Zhao, and Y. Zhang, "MomentDiff: Generative video moment retrieval from random to real," in *Annu. Conf. Neur. Inform. Process. Syst.*, 2023, pp. 65 948–65 966.
- [208] J. Lin, C. Gan, and S. Han, "TSM: Temporal shift module for efficient video understanding," in *IEEE Conf. Comput. Vis. Pattern Recog.*, 2019, pp. 7083–7093.
- [209] S. Mehta and M. Rastegari, "MobileViT: Light-weight, general-purpose, and mobile-friendly vision transformer," *arXiv preprint arXiv:2110.02178*, 2021.
- [210] C.-Y. Wu, Y. Li, K. Mangalam, H. Fan, B. Xiong, J. Malik, and C. Feichtenhofer, "MeMViT: Memory-augmented multiscale vision transformer for efficient long-term video recognition," in *IEEE Conf. Comput. Vis. Pattern Recog.*, 2022, pp. 13 587–13 597.
- [211] C. Zhang, D. Han, Y. Qiao, J. U. Kim, S.-H. Bae, S. Lee, and C. S. Hong, "Faster segment anything: Towards lightweight SAM for mobile applications," *arXiv preprint arXiv:2306.14289*, 2023.
- [212] J. Xu, Z. Xiong, and S. P. Bhattacharyya, "PIDNet: A real-time semantic segmentation network inspired by PID controllers," in *IEEE Conf. Comput. Vis. Pattern Recog.*, 2023, pp. 19 529–19 539.
- [213] R. Gao, "Rethinking dilated convolution for real-time semantic segmentation," in *IEEE Conf. Comput. Vis. Pattern Recog.*, 2023, pp. 4675–4684.
- [214] J. Wang and L. Ke, "LLM-Seg: Bridging image segmentation and large language model reasoning," in *IEEE Conf. Comput. Vis. Pattern Recog.*, 2024, pp. 1765–1774.
- [215] Y. Li, Z. Lai, W. Bao, Z. Tan, A. Dao, K. Sui, J. Shen, D. Liu, H. Liu, and Y. Kong, "Visual large language models for generalized and specialized applications," *arXiv preprint arXiv:2501.02765*, 2025.
- [216] H. Shi, S. D. Dao, and J. Cai, "LLMFormer: Large language model for open-vocabulary semantic segmentation," *Int. J. Comput. Vis.*, vol. 133, no. 2, pp. 742–759, 2025.
- [217] X. Lai, Z. Tian, Y. Chen, Y. Li, Y. Yuan, S. Liu, and J. Jia, "LISA: Reasoning segmentation via large language model," in *IEEE Conf. Comput. Vis. Pattern Recog.*, 2024, pp. 9579–9589.
- [218] Z. Xia, D. Han, Y. Han, X. Pan, S. Song, and G. Huang, "GSVA: Generalized segmentation via multimodal large language models," in *IEEE Conf. Comput. Vis. Pattern Recog.*, 2024, pp. 3858–3869.
- [219] Z. Chen, J. Wu, W. Wang, W. Su, G. Chen, S. Xing, M. Zhong, Q. Zhang, X. Zhu, L. Lu *et al.*, "InternVL: Scaling up vision foundation models and aligning for generic visual-linguistic tasks," in *IEEE Conf. Comput. Vis. Pattern Recog.*, 2024, pp. 24 185–24 198.
- [220] C. Ma, Y. Jiang, J. Wu, Z. Yuan, and X. Qi, "Groma: Localized visual tokenization for grounding multimodal large language models," in *Eur. Conf. Comput. Vis.*, 2024, pp. 417–435.
- [221] L. Chen, X. Wei, J. Li, X. Dong, P. Zhang, Y. Zang, Z. Chen, H. Duan, Z. Tang, L. Yuan *et al.*, "ShareGPT4Video: Improving video understanding and generation with better captions," in *Annu. Conf. Neur. Inform. Process. Syst.*, 2024, pp. 19 472–19 495.



Guohuan Xie is currently pursuing his B.E. degree at the College of Software, Nankai University, from 2022 to 2026. He is working with Prof. Yun Liu. His research interests include computer vision and machine learning.

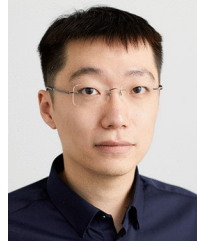


and label-efficient visual perception models.

Syed Ariff Syed Hesham is currently a Ph.D. candidate in Electrical and Electronic Engineering at Nanyang Technological University (NTU) in Singapore, and is also an A*STAR Computing and Information Science (ACIS) Research Scholar working under the Institute for Infocomm Research (I2R). He earned his Bachelor's degree in Electrical and Electronic Engineering from NTU in 2023. His research is at the intersection of deep learning and computer vision, with a particular focus on advancing effective



Wenya Guo received her B.E. and Ph.D. degrees from Nankai University in 2017 and 2022, respectively. Currently, she is a lecturer at the College of Computer Science, Nankai University. Her research interests include cross-modal alignment, sentiment computing and data-centric large language models.



Chapter Doctoral Dissertation Award. He served as area chair for ACL-ARR and PC members in various first-tier conferences, such as ICML, NeurIPS, AAAI, ICDE and ICLR.

Bing Li received the PhD degree from Northeastern University, China, in 2018. He is currently a professor with the University of Electronic Science and Technology of China. He was a senior scientist with A*STAR Centre for Frontier AI Research (CFAR), Singapore, and a research associate with the University of New South Wales, Australia. His research interests include intelligent information extraction, natural language processing, and machine learning. He is the awardee of the 2019 ACM China SIGMOD



Machine Intelligence and IEEE Transactions on Image Processing.

Ming-Ming Cheng (Senior Member, IEEE) received the PhD degree from Tsinghua University, in 2012, and then worked with Prof. Philip Torr in Oxford for 2 years. Since 2016, he is a full professor at Nankai University, leading the Media Computing Lab. His research interests include computer vision and computer graphics. He received awards, including ACM China Rising Star Award, IBM Global SUR Award, . He is a senior member of the IEEE and on the editorial boards of IEEE Transactions on Pattern Analysis and



Guolei Sun received his Ph.D. degree from ETH Zurich, Switzerland in 2024 and his master's degree from the King Abdullah University of Science and Technology (KAUST) in 2018. From 2018 to 2019, he was a Research Engineer with the Inception Institute of Artificial Intelligence, UAE. Currently, he is a professor at the College of Computer Science, Nankai University. His research interests include deep learning for classification, semantic segmentation, object counting, and weakly supervised learning.



Yun Liu received his B.E. and Ph.D. degrees from Nankai University in 2016 and 2020, respectively. Then, he worked with Prof. Luc Van Gool as a postdoctoral scholar at Computer Vision Lab, ETH Zurich, Switzerland. After that, he worked as a senior scientist at the Institute for Infocomm Research (I2R), A*STAR, Singapore. Currently, he is a professor at the College of Computer Science, Nankai University. His research interests include computer vision and machine learning.